Global Trajectory Optimisation: Can we prune the solution space when considering Deep Space Maneuvers?

Final Report

Authors: Joris T. Olympio, **Jean-Paul Marmorat**
Affiliation: Ecole des Mines de Paris, France

ESA Research Fellow/Technical Officer: **Dario Izzo**

Contacts:

Joris T. Olympio
Tel: (+33) (0)4 97 15 70 77
Fax: (+33) (0)4 97 15 70 66
e-mail: Joris.Olympio@ensmp.fr

Name of ESA's Research Fellow/Technical Officer
Tel: Telephone Number
Fax: +31(0)715658018
e-mail: act@esa.int

Available on the ACT website
http://www.esa.int/act

Ariadna ID: 06/4101
Study Duration: 6 months
Contract Number: 20274/06/NL/HE

Introduction and Motivations

Interplanetary optimization problems have always received a considerable attention in the trajectory optimization community. Present and past methods focused essentially on the use of local optimizers through the resolution of a two point boundary value problem (Maximum Principle), or through a parametric problem, either for low thrust or impulsive trajectory design.

Introducing swing-by maneuver can permit to reduce the value function. However the use of more and more swing-by bodies brings a mathematical challenge as the dimensionality of the problem increases.
This approach leads to such an increase in the number of local minima, that a global approach becomes imperative. Some works have already been done on the subject for the particular cases of direct multi – gravity assist trajectory (MGA) for the ballistic or the low thrust case.
However, MGA trajectory does not represent the general type of trajectory, since for impulsive trajectories, deep space maneuvers (DSM) have been proved to be of great use. Deep space maneuvers allow a gain of controllability and permit to reduce the consumption.

Multi gravity assist trajectory with Deep Space Maneuver (MGADSM) need more variables than the MGA case, and finding a global optimum become even more complex.
The best way to find the global optimum is to do a grid sampling. However these techniques are usually intractable, or very expensive. In order to simplify those costly algorithms, it is essential to prune the search space either with a set of constraints or with domain knowledge.

Our main objective is to find an automated approach that can reduce the computation cost of a search algorithm in order to provide MGADSM trajectories.

Study objectives

After the studies [2][3][4] considering the pruning of the search space for multi gravity assist trajectories, the problem is extended to the case where Deep Space Manoeuvres (DSM) are included between the gravity assists. The primary focus of the study is to assess the possibility of pruning part of the search space in case deep space manoeuvres are considered.

Although the subject is related to global optimization, few efforts are done on locating global optimum. Rather, we focus on how:

- Locating interesting sub-spaces of the decision vector space
- Performing efficient local optimization

A pruning policy would allow quickly finding a global optimum neighbourhood and thus limiting the resource needed to find a global optimum.

Local optimization techniques are helpful to tackle the global optimization problem. A stochastic initialization procedure combined with local optimization tools can provides a good set of locally optimal solutions. An element of this set can possibly be also a global optimum. Eventually, a specific step is needed to assess the global optimality of the solution founds.

Outline

The present report is decomposed into three parts:

1. The first part (chapter 1) is devoted to general description of the multi gravity assist problem considering deep space manoeuvres. Different Deep Space Manoeuvres model are described as well as swing-by models. We briefly investigate the complexity of the MGADSM problem in a strictly equivalent approach to GASP. We also describe reference test cases that will be use within the report.

2. The second part, including chapters 2 and 3, focuses on local optimization technique for the general multi gravity assist problem.
   We derive an optimal control problem using an indirect formulation. The key properties on the Primer Vector theory are recalled. The case of multiple DSM on a single leg is considered. The Primer Vector theory is then extended to the case considering intermediate swing-bys. Several examples of optimal MGADSM trajectory are presented.

3. The last part (chapter 4) is our pruning algorithm. It is an extension of the GASP algorithm to the DSM case. Only one DSM is considered per leg. The problem is then decoupled into several sub-problems. To optimise each sub-problems individually, the sub-problem decision vector is increased with specific variables which ensure that each sub-problem optimum is part of the overall problem optimum. The computational complexity is reduced, and polynomial.

List of Symbols

c	Coordination variable
g_0	Gravity constant ($g_0 = 9.806\ \mathrm{ms}^{-2}$)
I_{sp}	Specific impulse
m	Spacecraft mass
q	Mass flow rate
h	Swing-by periapsis altitude
r_p	Swing-by periapsis radius
$r_{\otimes}$	Planet position
$Q(\beta)$	Swing-by rotation matrix
r	Spacecraft position
t	Date or time
V , $V_{S/C}$	Spacecraft velocity
V_{in}	Swing-by incoming velocity
V_{out}	Swing-by outgoing velocity
$\mathbf{V}_{\infty}$	Hyperbolic excess velocity
V_{∞}	Hyperbolic excess velocity module
$\mathbf{X}$	State vector
μ	Gravitational constant ($\mu_{SUN} = 1.32712440018 \cdot 1e20\ \mathrm{m}^3\mathrm{s}^{-2}$)
ε	Relaxation parameter
η	Swing-by B-plane inclination.
$\boldsymbol{\lambda}$	Co state vector
$\boldsymbol{\lambda}_V$	Primer Vector
$\boldsymbol{\nu}$	Lagrange multiplier for constraints
$\Delta\mathbf{V}_0$	Departure velocity impulse
$\Delta\mathbf{V}_f$	Braking maneuver velocity impulse

Subscripts

$(\cdot)_0$, $(\cdot)_f$	value at initial and final time
$(\cdot)_i$	impulse number
$(\cdot)_{\cdot,k}$	phase or sub-problem number

Superscripts

$(\cdot)^*$	optimal state
$(\cdot)^+$	state after an impulse
$(\cdot)^-$	state before an impulse
$(\cdot)^i$	iteration number

Vectors are in **bold**.

1 Introduction

1.1 DSM models

1.1.1 Introduction

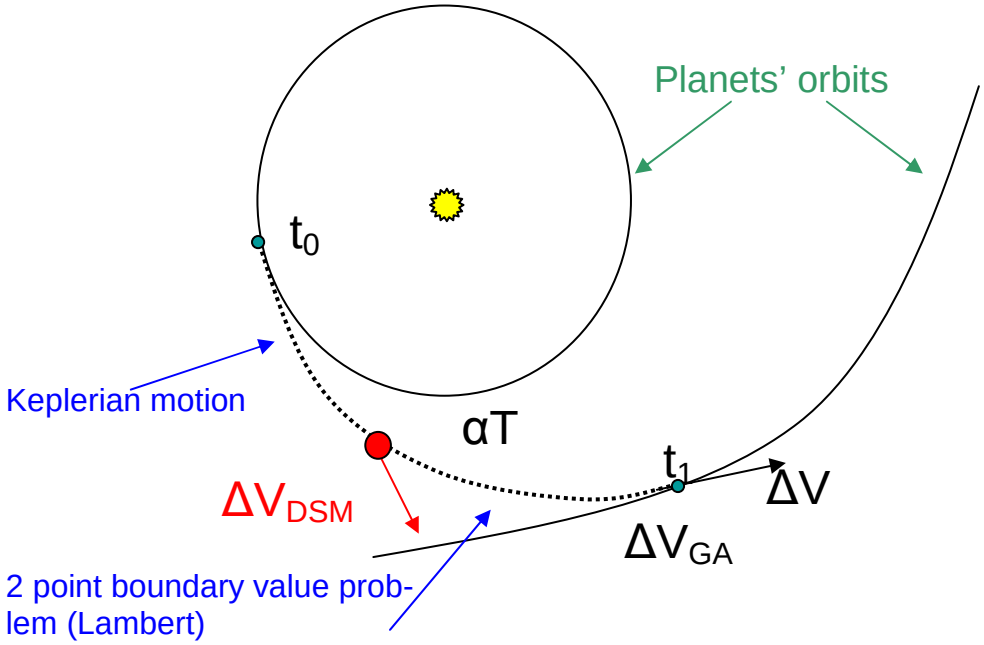

Figure 1. Trajectory illustration

A Deep Space Manoeuvre (DSM) is an impulsive manoeuvre. It represents change of velocity at a particular date and place of the space.
Since the location and date of a deep space maneuver are independent, it is described by at least 3 variables:

- Date of the maneuver
- Position of the DSM
- Velocity increment vector

There are different formulations that can be used. Indeed, any model that can give a full description of the DSM can be considered, but its description should have at least a 4 dimensional space description.

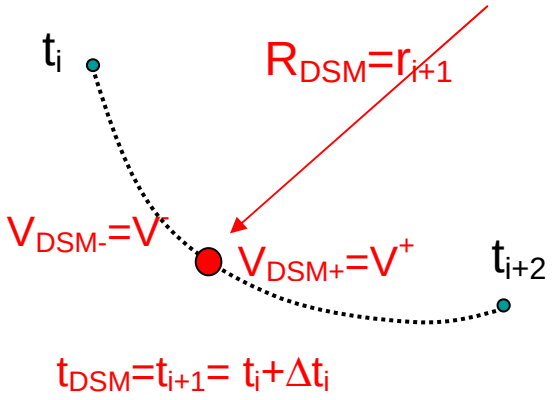

Figure 2. DSM model

1.1.2 Descriptions and DSM models

The DSM description and model is of particular importance. The choice of the variables has an influence on the convergence properties of the optimization algorithm.

Some models use:

- simplicity: some model only necessitates to solve an algebraic equation at each step, other requires integration.
- applicability: some model needs adding explicit constraints in the problem
- robustness: bounded or unbounded variables, …

The choice of the model is problem dependant. However, for global optimization algorithm simplicity and robustness are the most interesting feature.

The Date-Position model considers a point R_{DSM} from the space and a date t_{DSM}, where we apply an impulse ΔV_{DSM}.
The resolution of such a problem can be done through a formulation of 2 Lambert's problems [1] .

$$\begin{cases} Lambert\left(\mathbf{r}_i, \mathbf{r}_{i+1}, \Delta t_i\right) \rightarrow \mathbf{V}_i^+, \mathbf{V}_{i+1}^- \\ \Delta \mathbf{V}_{DSM} = \mathbf{V}_{i+1}^+ - \mathbf{V}_{i+1}^- \\ \mathbf{R}_{DSM} = \mathbf{r}_{i+1} \end{cases}$$

The Date-Velocity model uses only the information on the velocity increate and the date of the DSM. Since DSM trajectories are only composed of impulsive manoeuvres, the trajectory is a Keplerian trajectory almost everywhere. Thus, once every manoeuvres $\{t_i, \Delta\mathbf{V}_i\}$ are given and the initial state $[\mathbf{R}_0,\mathbf{V}_0, t_0]$ provided, one can propagate the initial state $[\mathbf{R}_0,\mathbf{V}_0+\Delta\mathbf{V}_0, t_0]$ from one impulsive manoeuvre date to the next. This propagation provides the full description of all the $[\mathbf{R}_i,\mathbf{V}_i, t_i]$.

$$\begin{cases} \dfrac{d\mathbf{v}}{dt} = -\dfrac{\mu}{\|\mathbf{r}\|^3}\mathbf{r}(t) \\ \mathbf{v}(0) = \mathbf{v}_i^+ \\ \dfrac{d\mathbf{r}}{dt} = \mathbf{v} \\ \mathbf{r}(0) = \mathbf{r}_i \end{cases} \tag{1.1}$$

And:

$$\begin{cases} \mathbf{r}_{i+1} = \mathbf{r}(\Delta t_i) \\ \mathbf{v}_{i+1}^- = \mathbf{v}(\Delta t_i) \\ \Delta\mathbf{V}_i = \mathbf{v}_{i+1}^+ - \mathbf{v}_{i+1}^- \end{cases} \tag{1.2}$$

Opposite to the Date-Position model, this model needs a constraint for the final position.

Table 1 summarizes the features of both models.

Table 1

	Date - Position	Date - Velocity
Variables	T, R_x, R_y, R_z	T, V_x, V_y, V_z
Constraints	on the swing-by altitude	on the final position on the swing-by altitude
Transfer resolution	Algebraic equation	Propagation + equation

Besides choosing between a position or a velocity description, the choice of the coordinates is also or importance. In this study, we mainly focus on Sun centered dynamics. The most suitable coordinates can be rectangular (or Cartesian), polar or spherical.
In rectangular coordinates, position and velocity are described by their natural values and provide a-priori unbounded variables. Only the expert point of view can limit the range for the different values.
In polar coordinates, the variables are amplitude, altitude and a polar angle. Again, this set of variable can only be bounded with expertise but for the angle variable which can be limited to the $[0,2\pi]$ interval.
The spherical coordinates provide the most interesting set of variables. These variables are the amplitude (radius or velocity amplitude), the azimuth angle α, and the elevation angle β. The angles α and β are limited respectively to $[0,2\pi]$ and $\left[-\frac{\pi}{2},\frac{\pi}{2}\right]$. The amplitude can also be restricted to the positive line R^+. An upper bound can be found with reasonable assumptions and expertise.

1.1.2.1 DSM swing-by description

The Date-Position and Date-Velocity models do not take into account the gravity assist feasibility, which express the maximum deviation on the hyperbolic excess velocity vector, according to the minimum allowed hyperbola pericenter altitude. Both models need an additional constraint for the swing-by minimum pericenter radius.

However, another description is possible. It accounts the gravity assist feasibility by assigning a variable to the altitude.
We have the following description vector:

$$\mathbf{X} = \begin{bmatrix} t & h & \eta \end{bmatrix}$$

Where t is the duration of the first coast arc, h is the altitude of the pericenter, and η is the B-plane inclination. The B-plane is perpendicular to the trajectory plane.
This approach however can only allow exactly one DSM per transfer leg. In addition, it is not suitable for direct transfer which does not include swing-bys.

1.2 Swing-By

1.2.1 Physical interpretation

Newton physics permits to explain the gravity assist phenomenon. During the encounter of a spacecraft with a planet, the sum of their kinetic energies before and after the encounter is the same, as is that of their linear momentum. But, during the encounter, the planet's gravitational interaction with the spacecraft produces a change in the velocity of the spacecraft. The eventual gain in kinetic energy of the spacecraft should be equal to the eventual loss in kinetic energy of the planet. Since the spacecraft mass is generally meaningless compared to the planet mass, the change in the planet velocity is usually meaningless too.

The trajectory of the spacecraft relative to the swing-by body is a hyperbola. The relative hyperbolic velocity is defined by:

$$\mathbf{V}_{\infty} = \mathbf{V}_{S/C} - \mathbf{V}_{\otimes} \tag{1.3}$$

This hyperbolic velocity is the same in module at the input and output of the gravisphere of the planet (e.g sphere of influence), for non powered swing-by.

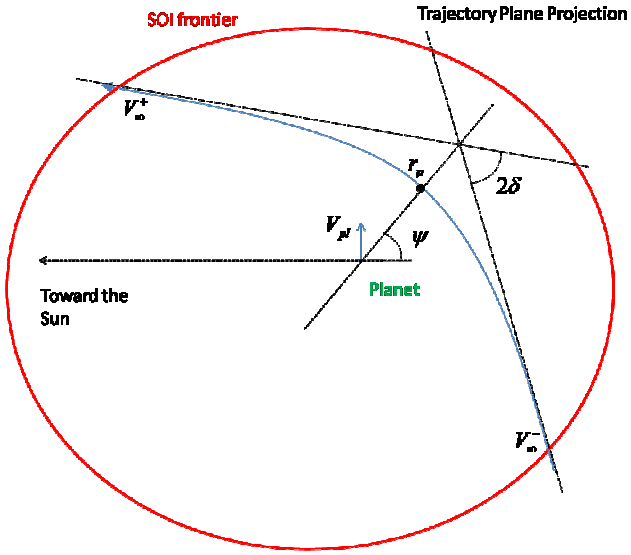

Figure 3. Swing-By model

In the literature, swing-bys are also referred as gravitational assistance, gravity assist, fly by, or also, but mistakenly to gravitational slingshot.

The physic can be simplified if we do not consider the dynamics of the spacecraft into the Sphere of Influence during the swing-by. The time of flight in the sphere of influence of the swing-by body is small compared to the total mission duration. Consequently, it is usually considered as a punctual phenomenon. Consequently, the perturbation maneuver is supposed instantaneous. This is often referred as the Patched Conic approximation.

1.2.2 Simplified Swing-By

Following the patched conic approximation, there is only a change of angle between $\boldsymbol{V}_\infty{}^+$ and $\boldsymbol{V}_\infty{}^-$. If we take 2δ the angle between $\boldsymbol{V}_\infty{}^+$ and $\boldsymbol{V}_\infty{}^-$ we get [1]:

$$\sin\delta = \frac{1}{1+\frac{r_p V_\infty{}^2}{\mu_2}} \tag{1.4}$$

Where r_p is the periapsis of the hyperbola during the encounter and μ_p is the gravitational constant of the swing-by body.
The rotation is done in the plane defined by the incoming relative velocity and the pericenter radius vector.

The velocity increase due to the swing-by is simply given by:

$$\Delta V = \left\| \mathbf{V}^+ - \mathbf{V}^- \right\| = 2V_\infty \sin\delta \tag{1.5}$$

There are limitations on δ and ΔV , given by the minimum radius which could not be lower than the planet radius, $r_{planet} < r_p$ and:

$$\sin\delta_{\max} = \frac{\mu}{\mu + r_{\min} V_\infty{}^2} \tag{1.6}$$

If $r_{planet} < r_p$, we say that the swing-by is feasible. The general constraints to respect, for a feasible swing-by, are then:

$$\psi = \begin{bmatrix} \dfrac{\mathbf{V}_\infty^{+T}\mathbf{V}_\infty^-}{\left\|\mathbf{V}_\infty^+\right\|\left\|\mathbf{V}_\infty^-\right\|} - \sin 2\delta \\ \left\|\mathbf{V}_\infty^+\right\| - \left\|\mathbf{V}_\infty^-\right\| \end{bmatrix} \tag{1.7}$$

The outgoing velocity vector from a swing-by can be calculated using:

$$\mathbf{V}_\infty^+ = \begin{bmatrix} V_{\infty x}{}^- & -\dfrac{V_\infty{}^- V_{\infty y}{}^-}{V_{\infty xy}^-} & -\dfrac{V_{\infty x}{}^- V_{\infty z}{}^-}{V_{\infty xy}^-} \\ V_{\infty y}{}^- & \dfrac{V_\infty{}^- V_{\infty x}{}^-}{V_{\infty xy}^-} & -\dfrac{V_{\infty y}{}^- V_{\infty z}{}^-}{V_{\infty xy}^-} \\ V_{\infty z}{}^- & 0 & V_{\infty xy}^- \end{bmatrix} \begin{bmatrix} \cos(2\delta) \\ \sin(2\delta)\cos\eta \\ \sin(2\delta)\sin\eta \end{bmatrix} \tag{1.8}$$

Where:

$$V_{\infty}^{-} = \left\| \mathbf{V}_{\infty}^{-} \right\|$$
$$V_{\infty xy}^{-} = \sqrt{\left(V_{\infty x}^{-}\right)^2 + \left(V_{\infty y}^{-}\right)^2}$$

And 2δ and η are respectively the deviation angle and the B-plane inclination with respect to the ecliptic.

1.2.3 Simplified Powered Swing-By model

If the gravity assist is not feasible, an impulsive maneuver permits to correct the hyperbola pericenter altitude. More specifically, in this study we can consider post-swing-by correction maneuver.
We apply the impulse after each gravity assist:

$$\Delta\mathbf{V} = \left(\mathbf{V}\left(t^{+}\right) - \mathbf{V}_{\otimes}(t)\right)\left(1 - \frac{\left\| \mathbf{V}_{\infty}^{-} \right\|}{\left\| \mathbf{V}\left(t^{+}\right) - \mathbf{V}_{\otimes}(t) \right\|}\right) \tag{1.9}$$

The gravity can be free if: $\left(V\left(t^{+}\right) - V_{\otimes}(t)\right) - V_{\infty}^{+} = 0$.

Placing a manoeuvre after the gravity assist, as expressed in the formula, allow considering the maximum available rotation of the hyperbolic velocity vector, without radius violation, and make a correction with an additional ΔV to match the heliocentric output velocity vector.

Thus, simply:

$$\Delta\mathbf{V} = \mathbf{V}\left(t^{+}\right) - \left(\mathbf{V}_{\otimes}(t) + \mathbf{V}_{\infty}^{+}\right) \tag{1.10}$$

Where $\mathbf{V}_{\infty}^{+}$ respects the maximum rotation constraint.

Another option would have been to place the impulse at the pericenter of the gravity assist. This would have been more efficient, but complexify the method.
This model has the advantage of decoupling the problem by considering several transfer arcs, where an arc is the patched legs joining 2 planets. This property, used in [2][3], allowed the MGA problem to have a polynomial space complexity.

1.2.4 Trajectory approximations

There are different models available:

- The Matched Conic approximation is one of the most accurate since it does not exhibit any velocity discontinuity in either velocity or position at the sphere of influence. The dynamics are integrated through the sphere of influence and outside, with appropriate jump conditions at the boundary of the sphere of influence when changing the referential from heliocentric to planetocentric and vice versa.

- The Patched Conic approximation has the same velocity property, it does not allow discontinuity in the velocity, but allows a discontinuity in the position at the sphere of influence. The position is considered to be the position of the planet.
- Other models exist like the mass less planet model which avoid the notion of sphere of influence. In the present study it is therefore the patched conic model which is of interest.

1.3 Impulsive Multi Gravity Assist problem

1.3.1 Problem Formulation

The problem is the one of finding the optimal impulses that allows reducing the characteristic velocity (ΔV budget) of a multi gravity assist trajectory.
The impulses are initially totally unknown, and possibly they may not be necessary.

The objective function to minimize for this problem can be written:

$$J = \left\|\Delta\mathbf{V}_0\right\| + \left\|\Delta\mathbf{V}_f\right\| + \sum_{i=1}^{n}\left\|\Delta\mathbf{V}_{DSM(i)}\right\| \tag{1.11}$$

With the initial conditions at the launch date t_0:

$$\mathbf{r}(t_0) = \mathbf{r}_0$$
$$\mathbf{v}(t_0) = \mathbf{v}_0$$

Under the constraints:

$$\psi_1(t_f) = \begin{bmatrix} \mathbf{r}(t_f) - \mathbf{r}_f \\ \left\|\mathbf{v}(t_f) - \mathbf{v}_f\right\| \\ t_f - t_0 - tof \end{bmatrix}$$
$$\psi_2(t_f) = \mathbf{r}(t_i) - \mathbf{r}_{B(i)}(t_i)$$

We give the gravity assists planet sequence $B = \{b_1, b_2, ..., b_N\}$ where b_i is a Solar system planet. The date of passage t_i at each b_i defines the mission scenario.

The dynamics is the spacecraft, under the sole Sun gravitational influence, is given by:

$$\begin{cases} \dfrac{d\mathbf{r}}{dt} = \mathbf{v} \\ \dfrac{d\mathbf{v}}{dt} = -\dfrac{\mu}{r^3}\mathbf{r} + q\dfrac{g_0 I_{sp}}{m}\mathbf{u} \\ \dfrac{dm}{dt} = -q \end{cases} \tag{1.12}$$

Where r defines the Cartesian position, v the velocity, μ the Sun gravitational constant, m the mass of the spacecraft, q the spacecraft fuel mass flow, Isp the specific impulse of the spacecraft thruster and u is the unit thrust direction.

The optimization variables are thus the date of encounter t_i with the planets, the Deep Space Maneuvers (DSM) model variables, and possibly the description of the swing-bys.

1.4 Problem complexity

1.4.1 Simple MGA problem complexity

According to [2][3], it is possible to have a polynomial complexity in space and time for the multi gravity Assist interplanetary transfer (MGA).

Indeed, this can be verified with the following assumptions:

- there is less than one revolution for each transfer: $N_i = 1$
- transfer directions are all in the same direction (posigrade or retrograde): $s_i = 1$
- launch window and mission phase time have the same discretization step.
- the Gravity Assist sequence is fixed.

This permits a grid sampling of the search space, and with the use of constraints, allows finding an optimum solution at a very low computational cost.

1.4.2 MGADSM problem complexity

As for the MGA problem, we can investigate the a-priori complexity of the extended problem using Deep Space Maneuvers (DSM). As this is the main motivation of this work, we can wonder if the GASP [2] approach also leads to a polynomial complexity.
As it has been written before, the model of a DSM need at least 4 independent variables.

Consider an n-GA trajectory with only one DSM per leg, and a launch window discretized into *k* bins of equal length, as well as each leg phase, from t_i to t_{DSMi} and t_{DSMi} to t_{i+1}
Thus:

1st phase:	1st leg	k^2
	2nd leg	$2k^2$
2nd phase:	1st leg	$3k^2$

	2nd leg	$4k^2$
nth phase:	1st leg	$(2n-1)k^2$
	2nd leg	$2nk^2$

This gives the sum:

$$C = \sum_{n=1}^{M} (4n-1)k^2$$

Or also:

$$C = k^2\left(4M^2 + M\right)$$

The space required for a *M* phases problem with one DSM per phase is of the order of $O(k^2)$. In addition, since all phases may not require a DSM, this computational cost may be pessimistic. The precedent approach can still be used on the time complexity.
Although the computational cost appears polynomial, the multiplicative factor $4M^2 + M$ should not be considered negligible. For example, a Cassini like mission, with up to 5 gravity assist, need a space of the order of $105k^2$.

However, the same approach cannot be followed for the space complexity. Opposite to date and planet positions in the MGA case, the positions and the date of the DSM are independent. Simple assumptions show that the space complexity is clearly not polynomial.
But we can benefit from the time complexity and appropriate local optimization methods to efficiently find a good trajectory. If our local methods prove to be efficient, the overall computational cost has great chance to be polynomial $O(k^n)$, where *n* still needs to be defined.

In addition, the MGA problem has an advantage over the MGADSM problem. In the MGA case we have a good description of the decision vector, as we only use the planet. In the MGADSM case, we are not sure if a DSM is necessary or not, which may need unpromising sampling of the search space.

For the MGA problem, each phase was described by a conic, and hence the sensitivity of the cost function with respect to the date and position of the planets is low compared to the full MGADSM case. Indeed, one can easily notice the difference in cost according to the place of the DSM. The size of the bins used to describe the DSM date must then be small compared to the phase time length.

1.5 References cases and examples of MGADSM trajectories

Along this report, we will consider mainly 3 test cases. Those are interplanetary transfer problems, known to be difficult. They are usually well referenced in the literature.
In most case, we only consider one DSM per leg.

1.5.1 Earth Venus Earth Jupiter

The EVEJ trajectory does not follow any missions, current or past.

Table 2.
EVEJ mission variables bounds

	Lower bound	Upper bound
Tref	01 Jan 2001	
T0 (days)	Tref -1000	Tref + 1000
tof (days)	0	1500
T_{dsm}/tof ratio	0.1	0.9
ΔV0 (m/s)	0	5000

1.5.2 Cassini Trajectory

Cassini spacecraft was launched on October 15, 1997 for a mission to Saturn and Titan. It is one of the most impressive missions, as the trajectory is one of the most complex one ever done for real. At the time of writing, Cassini should get an encounter with Titan in about 6 days.
Its trajectory has multiple swing-bys to reduce the fuel expenditure, but in addition several design constraint were given, such as the limited launch hyperbolic velocity due to an important mass budget of the spacecraft. There is also a constraint on the final velocity because the spacecraft need to get inserted into orbit around Saturn.

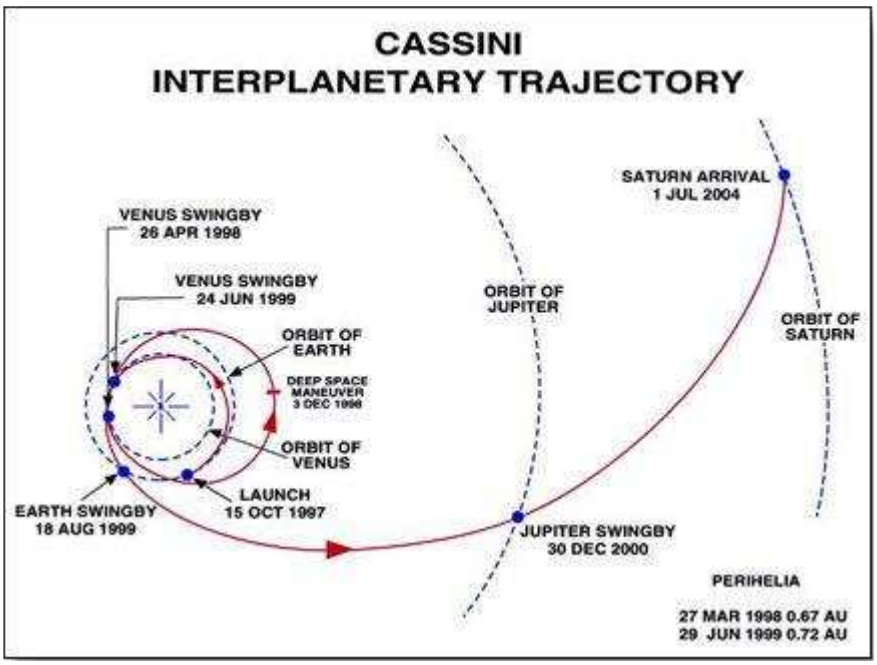

Figure 4. Cassini Mission (© NASA/JPL)

Table 3.
Original Cassini mission events[5]

Event	Date (days from T_0)	Real date	Velocities, altitudes

	[26]		
Launch	06/10/1997 (0)	15/10/1997	C_3 = 18.1 km²/s²
DSM1	16/03/1998 (162)	-	ΔV=0 m/s
Venus Swing-by	21/04/1998 (197)	27/04/1998	H=300km, V_∞=11.8 km/s
DSM2	02/12/1998 (423)	26/11/1998	ΔV=466 m/s
Venus Swing-by	20/06/1999 (622)	25/06/1999	H=2267km, V_∞=13 km/s
Earth Swing-by	16/08/1999 (679)	18/08/1999	H=500km, V_∞=19.1 km/s
Jupiter Swing-by	30/12/2000 (1181)	06/01/2001	H=139Js, V_∞=11.8 km/s
Phoebe flyby	12/06/2004 (2441)	-	D=52000km
Saturn Insertion	**01/07/2004 (2460)**	30/07/2004	ΔV=613 m/s
Titan flyby	27/12/2004 (2609)		H=1500 km, V_∞=5.9 km/s
End of Mission	01/07/2008 (3921)		

According to [5], the global optimum solutions need a C_3 between 35 and 55 km²/s², which is not possible in practice. There is thus a constraint on the initial launch velocity of about 4km/s.

In order to comply with the Cassini mission requirement, we set the following search box and constraint:

Table 4.
Cassini mission variables bounds

	ΔT_0[d, MJD2000]	ΔT_1[d]	ΔT_2[d]	ΔT_3[d]	ΔT_4[d]	ΔT_5[d]
Lower bound	-1000	100	100	30	400	800
Upper bound	0	400	500	300	1600	2200

1.5.3 ROSETTA mission

The ROSETTA mission purpose is to understand the origin of the Solar System. As the most primitive objects in our solar system, comets are good candidate for the ROSETTA mission. The mission was initially planned to rendezvous with comet 46P/Wirtanen but will eventually rendezvous with comet 67P/Churyumov-Geresimenko after a 10 years journey.

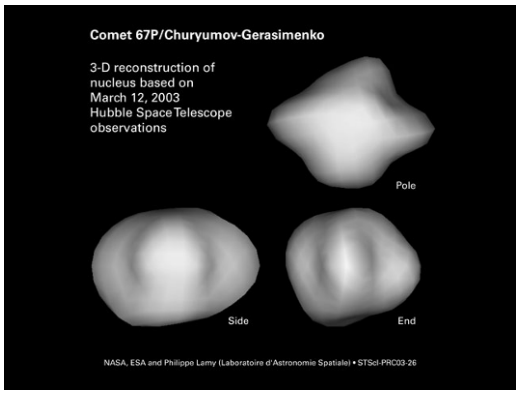

Figure 5. 3D view of the comet

The mission does not present any Deep Space Manoeuvre, but the trajectory is very complex with multiple Earth gravity assist, one Mars gravity assist and 2 comet flybys, before the final rendezvous.

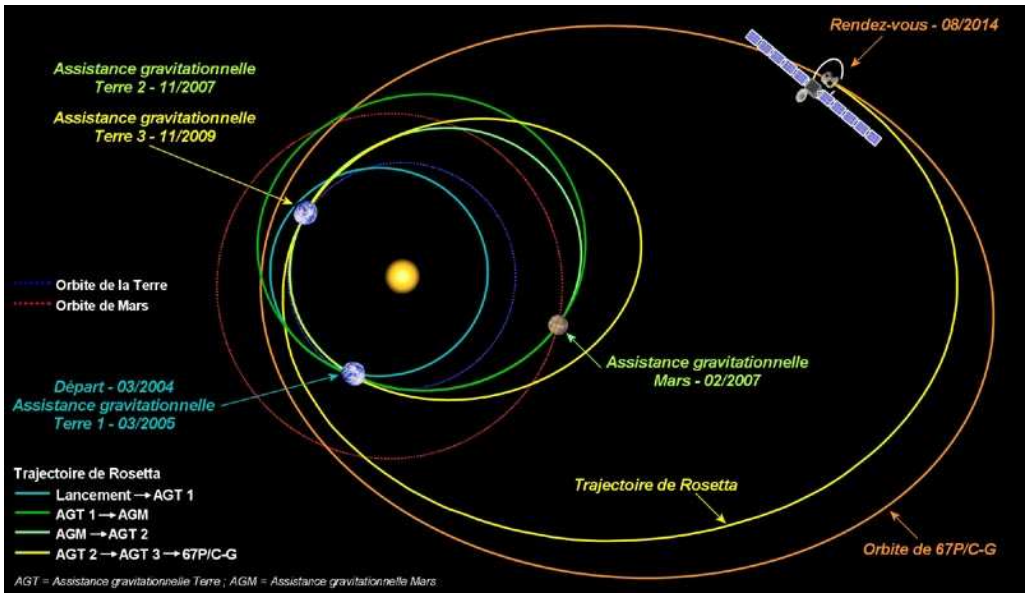

Figure 6. Rosetta trajectory (source: cnes.fr)

Table 5.
Original ROSETTA mission events[5] [6]

Event	**Date (days from T_0)** [26]	**Velocities, altitudes**
Launch	02/03/2004	3067kg, V_∞=3.515km/s
DSM 1	10/05/2004	158m/s
Earth SwingBy	04/03/2005 (367)	
DSM 2	28/09/2006	32m/s
Mars SwingBy	25/02/2007 (723)	2260m/s
DSM 3	25/04/2007	7 m/s
Earth SwingBy	13/11/2007 (261)	
Ast. Steins flyby	05/09/2008 (297)	
DSM 4	19/03/2009	7m/s
Earth SwingBy	13/11/2009 (434)	
Ast. Lutetia flyby	10/07/2010 (239)	
DSM 5	23/01/2011	789 m/s
Rendezvous	**22/05/2014 (1412)**	794 m/s
End of Mission	**../12/2015**	

The mission scenario was selected according to technical problem issue. As a consequence, swing-bys and flybys close to the sun were not allowed, and the launcher readiness was too risky for other scenario.

The DSM1 and DSM2 are actually called "ΔV gravity assist" by [6] as they permit to create Earth swing-by with an increased arrival velocity, compared to the others which only permit to flyby the selected asteroids.

Table 6.
ROSETTA mission events[5] optimized without DSM

Event	**Date (days from T_0)** [26]	**Velocities, altitudes**
Launch	02/03/2004	

Earth SwingBy	04/03/2005 (367)
Mars SwingBy	25/02/2007 (723)
Earth SwingBy	13/11/2007 (261)
Ast. Steins flyby	05/09/2008 (297)
Earth SwingBy	13/11/2009 (434)
Ast. Lutetia flyby	10/07/2010 (239)
Rendezvous	**../05/2014 (>1391)**
End of Mission	**../12/2015**

1.6 Final Remarks

We introduce the different DSM model and the swing-by model used in the patched conic approximation. These models are important because we will essentially refer to these one when computing a multi gravity assist with Deep Space Maneuver trajectory (MGADSM)

We also introduce the dynamics system which will be used later on to formulate the optimization problem.

We briefly investigate the cost function for a simple DSM case. This example gives us some insight about the behavior of the cost function, and the problem we might encounter, although the example was not by itself exhaustive.

In this study, we will try to take benefit of the recent promising results about the polynomial complexity of the MGA problem.

The following chapter deals with the well know Primer Vector theory. This theory will help us estimating the placement of the DSM, and give a good initial guess for the local solver.

2 Primer Vector theory

2.1 Introduction

The patched conic approximation leads to an interplanetary trajectory, by solving intermediate 2-body transfer problems. It is generally used for impulsive transfers; therefore the legs between each body along the trajectory are purely conics. According to Lambert's problem and Gibbs theory, the solutions to this problem are unique and easily computed.
When minimizing the characteristic velocity, it is possible to reduce the cost of the MGA solution, by considering additional intermediate impulses. The problem becomes more difficult. The search space is bigger and it is not an easy task to get a good initial guess.
Lawden theory brings us key elements to optimize a multiple impulse trajectories. It introduces a dual problem from the calculus of variation theory to seek the optimal impulses.

We will first introduce to the optimization problem, and provide a brief description of the Lawden Primer Vector theory. We will show how this theory can help us estimate the DSM position and amplitude. Also, an important feature of the theory is its ability to automatically find an optimum number of impulses. With this theoretical basis, we will introduce our search algorithm that manages to optimize any initial 2 impulses trajectory by adding optimal intermediate impulses.

2.2 Primer Vector Theory

2.2.1 Optimal control problem

Consider the problem of transferring a spacecraft from the state $\mathbf{X}(t_0) = [\mathbf{r_0}, \mathbf{v_0}, m_0]$ to the rendezvous conditions $[\mathbf{r_f}, \mathbf{v_f}]$ in a given time of flight $tof = t_f - t_0 > 0$. The spacecraft cartesian position and velocity vector and the spacecraft mass are given by the state vector is $\mathbf{X} = [\mathbf{r}, \mathbf{v}, m]$. The problem control variables comprise the mass flow rate q and the unit thrust direction $\boldsymbol{u}$. The spacecraft dynamics are given by:

$$\begin{cases} \dfrac{d\mathbf{r}}{dt} = \mathbf{v} \\ \dfrac{d\mathbf{v}}{dt} = -\dfrac{\mu}{r^3}\mathbf{r} + q\dfrac{g_0 I_{sp}}{m}\mathbf{u} \\ \dfrac{dm}{dt} = -q \end{cases} \tag{2.1}$$

Where r defines the Cartesian position, v the velocity, μ the Gravitationnal constant, m the mass of the spacecraft, q the fuel mass flow, Isp the specific impulse of the spacecraft thruster and u is the unit thrust direction.

In addition we have the following constraints on the control variables:

$$\begin{aligned} & q(q_{\max} - q) \geq 0 \\ & \|\mathbf{u}\| = 1 \end{aligned} \tag{2.2}$$

Such that we have a variable bounded mass flow rate $0 \leq q \leq q_{\max}$. Of course, for impulsive thrust we have either a thrusting force approaching infinity $q_{\max} \to \infty$ or a thrust time of the burns going to 0.

The objective function to maximize is:

$$J = -m(t_f) \tag{2.3}$$

Because of Tolstoïski formula, this is equivalent to minimize the characteristic velocity of the mission:

$$J = \|\Delta \mathbf{V}_f\| + \sum_{i=0}^{n} \|\Delta \mathbf{V}_i\| \tag{2.4}$$

Where *n* is the number of Deep Space Maneuvers (DSM), $\|\Delta \mathbf{V}_0\|$ is the initial impulse and $\|\Delta \mathbf{V}_f\|$ is the rendezvous manoeuvre impulse.

We introduce the Lagrange variables $\boldsymbol{\lambda} = [\boldsymbol{\lambda}_R, \boldsymbol{\lambda}_V, \lambda_m]$ for the state vector $\mathbf{X} = [\mathbf{R}, \mathbf{V}, m]$ and $\mu = [\mu_1, \mu_2]$ for the control constraints. We also introduce a slack variable α for handling the inequality constraints on the mass flow rate *q*. The Hamiltonian of the optimal control problem is:

$$\begin{aligned} H &= \boldsymbol{\lambda}_{\mathbf{R}}{}^T \frac{d\mathbf{r}}{dt} + \boldsymbol{\lambda}_{\mathbf{V}}{}^T \frac{d\mathbf{v}}{dt} + \lambda_m \frac{dm}{dt} + \mu_1 \left(q(q_{\max} - q) - \alpha^2 \right) + \mu_2 \left(\|\mathbf{u}\| - 1 \right) \\ &= q \left(\frac{\boldsymbol{\lambda}_{\mathbf{V}}{}^T g_0 I_{sp}}{m} \mathbf{u} + \mu_1 q_{\max} \right) + \boldsymbol{\lambda}_{\mathbf{R}}{}^T \frac{d\mathbf{r}}{dt} - \frac{\mu}{r^3} \boldsymbol{\lambda}_{\mathbf{V}}{}^T \mathbf{r} + \mu_2 \left(\|\mathbf{u}\| - 1 \right) + \mu_1 \left(q^2 - \alpha^2 \right) \end{aligned} \tag{2.5}$$

The necessary conditions of optimality permits to get the Lagrange variables equations:

$$\frac{\partial H}{\partial [\mathbf{u}, q, \alpha]} = 0$$

Thus:

$$\begin{cases} \dfrac{d\boldsymbol{\lambda}_{\mathbf{V}}}{dt} = -\boldsymbol{\lambda}_{\mathbf{R}} \\ \dfrac{d\boldsymbol{\lambda}_{\mathbf{R}}}{dt} = G(t, \mathbf{r}) \boldsymbol{\lambda}_{\mathbf{V}} \end{cases} \tag{2.6}$$

The Maximum Principle gives the optimal control, which is:

$$\mathbf{u}^* = \frac{\boldsymbol{\lambda}_\mathbf{v}}{\|\boldsymbol{\lambda}_\mathbf{v}\|} \text{ if } q \neq 0 \text{ and } \mu_2 \neq 0 \tag{2.7}$$

The vector $\boldsymbol{\lambda}_\mathbf{v}$ is called the primer vector, and it is the co-state of the velocity.
The 3×3 gradient gravity matrix *G* for two-body motion along a reference orbit $(t,\mathbf{r})$ is given by [1]:

$$\mathbf{G}(t,\mathbf{r}) = \frac{\mu}{\|\mathbf{r}\|^5}\left(3\mathbf{r}\cdot\mathbf{r}^T - \|\mathbf{r}\|^2\mathbf{I}_d\right)$$

This matrix is usually evaluated around a reference trajectory, as (2.1) and (2.7) cannot be integrated concurrently (see 2.5.1.1).
Note also:

$$\mathbf{g}(t) = -\frac{\mu}{\|\mathbf{r}\|^3}\mathbf{r}(t)$$

We can then introduce the switching function *S*:

$$H = qS + \boldsymbol{\lambda}_\mathbf{R}{}^T\frac{d\mathbf{r}}{dt} - \frac{\mu}{r^3}\boldsymbol{\lambda}_\mathbf{V}{}^T\mathbf{r} + \mu_2\left(\|\mathbf{u}\|-1\right) + \mu_1\left(q^2-\alpha^2\right) \tag{2.8}$$

With:

$$S = \frac{g_0 I_{sp}}{m}\left(\boldsymbol{\lambda}_\mathbf{V}{}^T\mathbf{u} + \frac{\mu_1 q_{\max} m}{g_0 I_{sp}}\right) \tag{2.9}$$

The switching function permits to describe the instant of switching of the control.

And for the optimal control $\mathbf{u}^*$, $S = S*$:

$$\begin{cases} S > 0 \Rightarrow q = q_{\max} \\ S < 0 \Rightarrow q = 0 \\ S = 0 \Rightarrow \text{singular control} \end{cases}$$

Indeed, for the impulsive case, we have either a maximum thrust arc of a null thrust arc. Intermediate thrust arcs (singular arc) only permit to get variable thrust.

2.2.1.1 General Application of Primer Vector Theory

If we now study the case where we have an impulse. The switching function *S* crosses zero.
We have then:

$$\begin{cases} H\left(t_i^-\right) - H\left(t_i^+\right) = 0 \\ \mathbf{r}\left(t_i^-\right) - \mathbf{r}\left(t_i^+\right) = 0 \end{cases} \tag{2.10}$$

This implies that the primer vector is perpendicular to its derivative: $\boldsymbol{\lambda}_{\mathbf{V}} \perp \boldsymbol{\lambda}_{\mathbf{R}}$.
And:

$$\begin{cases} \dfrac{dS}{dt} = \dfrac{g_0 I_{sp}}{m} \dfrac{d}{dt} \left\| \boldsymbol{\lambda}_{\mathbf{v}} \right\| \\ \dfrac{d}{dt} \left\| \boldsymbol{\lambda}_{\mathbf{v}} \right\| = 0 \end{cases}$$

Integrating this last equation gives:

$$S = \frac{g_0 I_{sp}}{m} \left(\left\| \boldsymbol{\lambda}_{\mathbf{v}} \right\| + cnst_1 \right)$$

The constant $cnst_1$ is the normalization constant of $\boldsymbol{\lambda}_{\mathbf{v}}$ or also the magnitude of $\left\| \boldsymbol{\lambda}_{\mathbf{v}} \right\|$ for all impulses. We can choose to unit $\left\| \boldsymbol{\lambda}_{\mathbf{v}} \right\|$ at impulses.

Now, following the approach of Jezewski [7], we investigate the case where we need to add an impulse. Adding a new impulse $\Delta \mathbf{V}_{n+1}$ perturbs the nominal trajectory. We get the new value function:

$$J = \left\| \Delta \mathbf{V}_0 + \delta \mathbf{V}_0 \right\| + \left\| \Delta \mathbf{V}_f - \delta \mathbf{V}_f \right\| + \sum_{i=1}^{n} \left\| \Delta \mathbf{V}_i + \delta \mathbf{V}_i^+ - \delta \mathbf{V}_i^- \right\| + \left\| \Delta \mathbf{V}_{n+1} \right\| \tag{2.11}$$

The relative change in the value function due to adding the new impulse is then:

$$dJ = \frac{\Delta \mathbf{V}_0{}^T \delta \mathbf{V}_0}{\left\| \Delta \mathbf{V}_0 \right\|} - \frac{\Delta \mathbf{V}_f{}^T \delta \mathbf{V}_f}{\left\| \Delta \mathbf{V}_f \right\|} + \sum_{i=1}^{n} \frac{\Delta \mathbf{V}_i{}^T \left(\delta \mathbf{V}_i^+ - \delta \mathbf{V}_i^- \right)}{\left\| \Delta \mathbf{V}_i \right\|} + \left\| \Delta \mathbf{V}_{n+1} \right\| + o\left(\left\| \delta \mathbf{V}_0 \right\|, \left\| \delta \mathbf{V}_f \right\|, \left\| \delta \mathbf{V}_i \right\| \right)$$

This expression can be rewritten to first order:

$$dJ = \boldsymbol{\lambda}_{V0}{}^T \delta \mathbf{V}_0 - \boldsymbol{\lambda}_{Vf}{}^T \delta \mathbf{V}_f + \sum_{i=1}^{n} \frac{\Delta \mathbf{V}_i{}^T \left(\delta \mathbf{V}_i^+ - \delta \mathbf{V}_i^- \right)}{\left\| \Delta \mathbf{V}_i \right\|} + \left\| \Delta \mathbf{V}_{n+1} \right\| \tag{2.12}$$

Because the Hamiltonian is constant over each leg linking two successive impulses, the 2 first terms on the right hand side can be related to the intermediate impulses with the use of the primer vector and relative perturbation $\delta \mathbf{r}$ of the impulses position.

$$\left[\boldsymbol{\lambda}_V{}^T \delta \mathbf{v} + \boldsymbol{\lambda}_r{}^T \delta \mathbf{r} \right]_i^{i+1} = 0$$

The first term of (2.10) vanishes because of the Hamiltonian and the position trajectory continuity, and:

$$dJ = \left\| \delta \mathbf{V}_{n+1}^{-} - \delta \mathbf{V}_{n+1}^{+} \right\| \left(1 - \boldsymbol{\lambda}_{Vn+1}{}^{T} \frac{\delta \mathbf{V}_{n+1}^{-} - \delta \mathbf{V}_{n+1}^{+}}{\left\| \delta \mathbf{V}_{n+1}^{-} - \delta \mathbf{V}_{n+1}^{+} \right\|} \right) \tag{2.13}$$

For example, if $\left\| \boldsymbol{\lambda}_{Vn+1} \right\|$ exceeds unity, then the differential cost becomes negatives and we can reduce the cost.

2.2.2 Conditions for a primer optimal trajectory

According to the former development, we have 4 conditions for a ballistic trajectory to be optimal [7]. They are resumed below.

Property 2.1:

1. *the primer vector and its derivative should be continuous*
2. *if there is an impulse, the primer vector is aligned with the impulse, and its module is 1.*
3. *the primer vector module should not exceed 1.*
4. *the derivative of all intermediate impulse is zero.*

It is important to emphasize one of the major drawbacks of Lawden theory. In order to optimize a trajectory it is necessary to have at least 2 impulses. More precisely, we can only compute trajectory where we can evaluate the boundaries (or the transversality conditions).
To compute the primer vector history, it is thus important to evaluate its value at one boundary.

2.3 Boundary conditions

2.3.1 Calculus of Variation

From the value function J (2.3) and general boundary constraints ψ, we can construct the performance index:

$$L(\mathbf{x}, \mathbf{u}, \boldsymbol{\Lambda}) = J + \boldsymbol{\nu}^{T} \cdot \boldsymbol{\psi}\left(\mathbf{x}(t_f)\right) + \int_{t_0}^{t_f} \boldsymbol{\Lambda}^{T} \cdot \left(f(\mathbf{x}, \mathbf{u}; t) - \frac{d\mathbf{x}}{dt} \right) dt \tag{2.14}$$

Where $f(x,t)$ is the problem state dynamical equation, Λ is the costate vector and ν is the Lagrange multiplier associated to the constraints.

With:

$$\boldsymbol{\Lambda} = \begin{bmatrix} \boldsymbol{\lambda}_R \\ \boldsymbol{\lambda}_V \end{bmatrix}, \ \mathbf{X} = \begin{bmatrix} \mathbf{r} \\ \mathbf{v} \end{bmatrix} \text{ and } f(\mathbf{X}(t)) = \begin{bmatrix} \mathbf{v}(t) \\ \mathbf{g}(\mathbf{r}(t)) \end{bmatrix}$$

The state vector ***X*** includes the position vector ***r*** of the spacecraft according to the central/reference body position, the velocity ***v*** of the spacecraft according to the reference frame.

The first differential becomes:

$$\begin{aligned}
dL = & dJ + ... \\
& + \psi\left(\mathbf{X}\left(t_f\right)\right)^T \cdot d\mathbf{v} + \mathbf{v}^T \cdot d\boldsymbol{\psi}\left(\mathbf{X}\left(t_f\right)\right) + ... \\
& + \boldsymbol{\lambda}_V\left(t_f\right) d\mathbf{V}_f - \boldsymbol{\lambda}_V\left(t_0\right) d\mathbf{V}_0 + ... \\
& + \int_{t_0}^{t_1^-} \left[\left(\boldsymbol{\lambda}_R + \frac{d\boldsymbol{\lambda}_V}{dt} \right) \cdot \delta\mathbf{v} + \left(\boldsymbol{\lambda}_V \frac{\partial \mathbf{G}}{\partial \mathbf{r}} + \frac{d\boldsymbol{\lambda}_R}{dt} \right) \cdot \delta\mathbf{r} \right] dt + ... \\
& + \int_{t_i^+}^{t_f} \left[\left(\boldsymbol{\lambda}_R + \frac{d\boldsymbol{\lambda}_V}{dt} \right) \cdot \delta\mathbf{v} + \left(\boldsymbol{\lambda}_V \frac{\partial \mathbf{G}}{\partial \mathbf{r}} + \frac{d\boldsymbol{\lambda}_R}{dt} \right) \cdot \delta\mathbf{r} \right] dt + ... \\
& + \sum_{i=1}^{n} \left\{ dL_{R_i} + dL_{t_i} dt + dI_i \right\}
\end{aligned} \tag{2.15}$$

And for conciseness:

$$\begin{aligned}
L_{R_i} &= \boldsymbol{\lambda}_R{}^T\left(t^-\right) d\mathbf{R}_i^- - \boldsymbol{\lambda}_R{}^T\left(t^+\right) d\mathbf{R}_i^+ \\
L_{t_i} &= \left(\boldsymbol{\lambda}_V{}^{+T} \frac{d\mathbf{V}^+}{dt} + \boldsymbol{\lambda}_R{}^{+T} \frac{d\mathbf{R}^+}{dt} \right) - \left(\boldsymbol{\lambda}_V{}^{-T} \frac{d\mathbf{V}^-}{dt} + \boldsymbol{\lambda}_R{}^{-T} \frac{d\mathbf{R}^-}{dt} \right) \\
dI_i &= \int_{t_i^+}^{t_{i+1}^-} \left[\left(\boldsymbol{\lambda}_R + \frac{d\boldsymbol{\lambda}_V}{dt} \right)^T \cdot \delta\mathbf{v} + \left(\boldsymbol{\lambda}_V{}^T \frac{\partial \mathbf{G}}{\partial \mathbf{r}} + \frac{d\boldsymbol{\lambda}_R}{dt} \right)^T \cdot \delta\mathbf{r} \right] dt
\end{aligned} \tag{2.16}$$

Where *n* is the number of DSM, $\{t_i\}_{i=1..n}$ are the date of the DSM, $t_{n+1}^- = t_f$.
If there is no DSM, the last term vanishes and $t_i = t_i^+ = t_i^-$.

2.3.2 Boundary constraints handling

2.3.2.1 Rendezvous problem

The rendezvous is given by the conditions:

$$\begin{aligned}
\mathbf{r}\left(t_f\right) &= \mathbf{r}_f \\
\mathbf{v}\left(t_f\right) &= \mathbf{v}_f
\end{aligned}$$

There are no constraints: $\psi = 0$.
Thus:

$$\frac{\partial J}{\partial \mathbf{V}_0} = \frac{\Delta \mathbf{V}_0}{\left\| \Delta \mathbf{V}_0 \right\|}$$
$$\frac{\partial J}{\partial \mathbf{V}_f} = -\frac{\Delta \mathbf{V}_f}{\left\| \Delta \mathbf{V}_f \right\|} \tag{2.17}$$

where $\Delta \mathbf{V}_0 = \mathbf{V}_0 - \mathbf{V}_{\otimes 0}$ and $\Delta \mathbf{V}_f = \mathbf{V}_{\otimes f} - \mathbf{V}_f$

Then, to get an optimum point we should get:

$$\boldsymbol{\lambda}_{\mathbf{V}}(t_0) = \frac{\Delta \mathbf{V_0}}{\left\| \Delta \mathbf{V_0} \right\|} \tag{2.18}$$

$$\boldsymbol{\lambda}_{\mathbf{V}}(t_f) = \frac{\Delta \mathbf{V}_f}{\left\| \Delta \mathbf{V}_f \right\|} \tag{2.19}$$

Note that the position constraints are implicitly satisfied since the trajectory is a solution of a Lambert's problem.

2.3.2.2 Constraint on the initial velocity

Consider the initial constraint:

$$\psi(t_0) = \left\| \mathbf{V_0} - \mathbf{V}(t_0) \right\| - V_\infty \tag{2.20}$$

Differentiating ψ gives:

$$d\psi = \frac{\mathbf{V}_0 - \mathbf{V}_{\otimes 0}}{\left\| \mathbf{V}_0 - \mathbf{V}_{\otimes 0} \right\|} d\mathbf{V}_0 \tag{2.21}$$

The stationnarity of the Lagrangian (2.13) permits to get the initial condition on the primer vector:

$$\boldsymbol{\lambda}_{\mathbf{V}}(t_0) = \nu \frac{\mathbf{V_0} - \mathbf{V}_{\otimes 0}}{\left\| \mathbf{V_0} - \mathbf{V}_{\otimes 0} \right\|} \tag{2.22}$$

Where ν is the Lagrange scalar associated to the constraint ψ.

The same expression can be calculated for a constraint on the final velocity. Thus we simply have in this case:

$$\boldsymbol{\lambda}_{\mathbf{V}}(t_f) = -\nu \frac{\mathbf{V}_f - \mathbf{V}_{\otimes f}}{\left\| \mathbf{V}_f - \mathbf{V}_{\otimes f} \right\|} \tag{2.23}$$

Where ν is the Lagrange scalar associated to the constraint ψ.

These expressions (2.18, 2.19) will be useful when considering MGA-DSM primer optimal trajectories (see 3).

2.4 Optimizing with the Primer vector

2.4.1 Solution initial guess

If a multiple impulse trajectory is not Primer optimal and need to be optimized, a good starting guess is to use the time where the primer is maximum. This guess is actually good to first order, for improving the reference trajectory.

Jezewski [7] proposes an approach which estimates the error in position. However, this approach is only valid when the linear developments are respected.

$$dR_i = cA^{-1} \frac{\boldsymbol{\lambda}_{v_i}}{\left\| \boldsymbol{\lambda}_{v_i} \right\|} \tag{2.24}$$

With:

$$A = \Phi_4(t_i, t_f)\Phi_2^{-1}(t_i, t_f) - \Phi_4(t_i, t_0)\Phi_2^{-1}(t_i, t_0) \tag{2.25}$$

And:

$$c = \frac{\left\| \Delta\mathbf{V}_0 \right\| \left\| \Delta\mathbf{V}_f \right\| \left(\beta^T \boldsymbol{\lambda}_f - \boldsymbol{\alpha}^T \boldsymbol{\lambda}_0 - 1 \right)}{\left\| \Delta\mathbf{V}_f \right\| \left(\left\| \boldsymbol{\alpha} \right\|^2 - \left(\boldsymbol{\alpha}^T \boldsymbol{\lambda}_0 \right)^2 \right) + \left\| \Delta\mathbf{V}_0 \right\| \left(\left\| \boldsymbol{\beta} \right\|^2 - \left(\boldsymbol{\beta}^T \boldsymbol{\lambda}_f \right)^2 \right)} \tag{2.26}$$

Where:

$$\boldsymbol{\lambda}_0 = \frac{\Delta\mathbf{V}_0}{\left\| \Delta\mathbf{V}_0 \right\|}$$

$$\boldsymbol{\lambda}_f = \frac{\Delta\mathbf{V}_f}{\left\| \Delta\mathbf{V}_f \right\|}$$

$$\boldsymbol{\alpha} = \Phi_2^{-1}(t_i, t_0) A^{-1} \frac{\boldsymbol{\lambda}_{v_i}}{\left\| \boldsymbol{\lambda}_{v_i} \right\|}$$

$$\boldsymbol{\beta} = \Phi_2^{-1}(t_i, t_f) A^{-1} \frac{\boldsymbol{\lambda}_{v_i}}{\left\| \boldsymbol{\lambda}_{v_i} \right\|}$$

The scalar *c* is the magnitude of the intermediate impulse.

2.4.2 Algorithm

The primer vector approach for the optimization of interplanetary trajectory presents a number of disadvantages.
Indeed, we cannot integrate the primer vector and the state dynamics simultaneously with the initial condition $\mathbf{X}(t_0) = \{\mathbf{R}_0, \mathbf{V}_0\}$ and $\boldsymbol{\Lambda}(t_0) = \left\{\boldsymbol{\lambda}_0, \dot{\boldsymbol{\lambda}}_0\right\}$, and solve the TPBVP to find an optimal trajectory, for the following reasons:

- the number of impulses is unknown and may vary from one iteration to another.
- the amplitude of the impulses are unknown, and since we do not know the number of impulse, the dimension of the search space may change from one iteration to the next.
- the impulses impose a discontinuity on the velocity and hence the computation of the trajectory is numerically extremely sensitive.

Note also, that the calculus of variation theory cannot provide the DSM amplitude. This is because the mass flow rate is a linear term in (2.9), and we are considering an impulsive control.

The algorithms presented avoid these difficulties. We proceed in 2 stages. We first compute the trajectory with the known control (impulses) by using a Lambert's problem formulation or integrating the state equations. Once the trajectory is computed, we can integrate the co-state equation along the state trajectory using the appropriate boundary conditions (see 2.3) on the primer vector.
With 2.2.2, the primer vector history informs us about the optimality of the trajectory. We also have an information of the optimal number of impulse for the current nominal trajectory. Note that we can provide information on the gradient.

The algorithm (Table 7) consists of locally optimizing a trajectory using the initial/estimated guess given by the primer vector. After each local optimization, we check the criterions of optimality and loop with a new initial guess if they are not satisfied.

Table 7. Algorithm

Step 1. Compute the trajectory $\mathbf{X}(t) = \{\mathbf{R}(t), \mathbf{V}(t)\}$
Step 2. Evaluate Primer Vector $\boldsymbol{\lambda}(t)$
Step 3. If optimality criterions are satisfied, stop Otherwise, estimate the number of DSM, R_{DSM} and t_{DSM}, and

return to Step 1.

2.4.3 Comments on the algorithm

The primer vector history is only computed once per iteration, and Lawden theory is only used as a verification and estimation tool, which is critical to ensure the convergence of the algorithm.

In order, to improve convergence, we do not allow reducing the number of DSM during the process, but instead, each maximum (above or under 1) are considered as potential impulses.

It is important to mention that for multi-revolution transfer, the primer vector tends to add one or two impulse per revolution, such that the Lambert solver is always looking for less than one revolution solutions. There is no need to specify the number of revolution or the branch to select in the Lambert's problem solver.

Numerical issue
The primer vector theory suffers of singularities [8]. In addition, when the very first impulse is almost 0, it is numerically tricky to compute $\frac{\Delta\mathbf{V_0}}{\|\Delta\mathbf{V_0}\|}$. As the formulation needs initial and final boundary value for the primer vector $\boldsymbol{\lambda}_V$, we can consider to switch from the impulse $\Delta\mathbf{V}_0$ to the first DSM impulse $\Delta\mathbf{V}_1$. Indeed, for a rendezvous problem, if $\mathbf{r_0} \neq \mathbf{r}_f$ we must have $J > \|\Delta\mathbf{V}_2\|$ such that we have at least 2 impulses in the trajectory. The primer vector history is then always well defined.

2.5 Numerical Analysis

2.5.1 Primer Vector Computation

2.5.1.1 TPBVP approach

For a transfer problem from $\mathbf{r}(t_0) = \mathbf{r_0}$ to $\mathbf{r}(t_f) = \mathbf{r_f}$, under the dynamics given by (2.1) and (2.4), a Two Point Boundary Value Problem (TPBVP) can be formulated as follow:

$$\begin{cases} \dfrac{d\mathbf{r}}{dt} = \mathbf{v} \\ \dfrac{d\mathbf{v}}{dt} = \mathbf{g}(t,\mathbf{r}) \\ \dfrac{d\boldsymbol{\lambda}_{\mathbf{R}}}{dt} = \mathbf{G}(t,\mathbf{r})\boldsymbol{\lambda}_{\mathbf{V}} \\ \dfrac{d\boldsymbol{\lambda}_{\mathbf{V}}}{dt} = -\boldsymbol{\lambda}_{\mathbf{R}} \\ \mathbf{r}(t_0) = \mathbf{r_0}, \mathbf{r}(t_f) = \mathbf{r_f} \\ \|\boldsymbol{\lambda}_V(t_0)\| = 1, \|\boldsymbol{\lambda}_V(t_f)\| = 1 \end{cases} \tag{2.27}$$

We can get the primer vector history using any two point boundary value (TPBVP) solver. A shooting method or a collocation technique can solve (2.9).

2.5.1.2 Transition matrix approach

Another approach is to consider the use of transition matrix. This allows calculating the solution of a linear TPBVP. In this case the trajectory must be known beforehand. This is done by the appropriate use of a Lambert's problem solver. Once the state trajectory is known, the co state dynamical equations can be linearized around the state trajectory.

Let's briefly recall the symplectic property of the transition matrix [1]:

$$\Phi^T J \Phi = J \text{ where } J = \begin{bmatrix} 0 & I \\ -I & 0 \end{bmatrix}$$

And also:

$$\Phi = \begin{bmatrix} \Phi_1 & \Phi_2 \\ \Phi_3 & \Phi_4 \end{bmatrix}$$

$$\Phi^{-1} = \begin{bmatrix} \Phi_4 & -\Phi_2 \\ -\Phi_3 & \Phi_1 \end{bmatrix}$$

$$\Phi^{-1}(t,t_0) = \Phi(t_0,t)$$

Equation (2.12) can then also be written:
Thus:

$$\begin{cases} \mathbf{x}(t) = lambert(\mathbf{r_0}, \mathbf{r_f}, t_0, t_f) \\ \boldsymbol{\lambda}_{\mathbf{V}}(t_0) = \dfrac{\Delta \mathbf{V_0}}{\|\Delta \mathbf{V_0}\|} \\ \boldsymbol{\lambda}_R(t_0) = \Phi_2^{-1}(t_f, t_0)\left(\boldsymbol{\lambda}_{\mathbf{V}}(t_f) - \Phi_1(t_f, t_0)\boldsymbol{\lambda}_V(t_0)\right) \\ \dfrac{d\boldsymbol{\lambda}_{\mathbf{R}}}{dt} = G(t, \mathbf{r})\boldsymbol{\lambda}_{\mathbf{V}} \\ \dfrac{d\boldsymbol{\lambda}_{\mathbf{V}}}{dt} = -\boldsymbol{\lambda}_{\mathbf{R}} \end{cases} \tag{2.28}$$

Where:

$$\begin{cases} \dfrac{d\Phi}{dt}(t, t_0) = \begin{pmatrix} 0 & -I_{3\times 3} \\ \mathbf{G}(t) & 0 \end{pmatrix} \Phi(t, t_0) \\ \Phi(t_0, t_0) = I \end{cases} \tag{2.29}$$

In this case, one can integrate (2.13) and (2.14) concurrently, and then compute the primer vector.

2.5.2 Computation of the gradient

The results of Jezewski [7] can be extended to N-DSM trajectories [9]. Then:

$$\begin{cases} \dfrac{\partial J}{\partial t_{DSMi}} = \dfrac{d\boldsymbol{\lambda}}{dt}^{+T} \mathbf{V}^{+} - \dfrac{d\boldsymbol{\lambda}}{dt}^{-T} \mathbf{V}^{-} \\ \dfrac{\partial J}{\partial \mathbf{X}_{DSMi}} = \dfrac{d\boldsymbol{\lambda}}{dt}^{+} - \dfrac{d\boldsymbol{\lambda}}{dt}^{-} \end{cases} \tag{2.30}$$

And:

$$\nabla J = \left[\frac{\partial J}{\partial t_{DSM(1)}} \quad \cdots \quad \frac{\partial J}{\partial t_{DSM(n)}} \quad \frac{\partial J}{\partial \mathbf{X}_{DSM(1)}} \quad \cdots \quad \frac{\partial J}{\partial t_{DSM(n)}} \right]$$

The state transition matrices can also be used to compute the gradient, as it will be explained in the next section.

2.5.3 Simple study of optimality

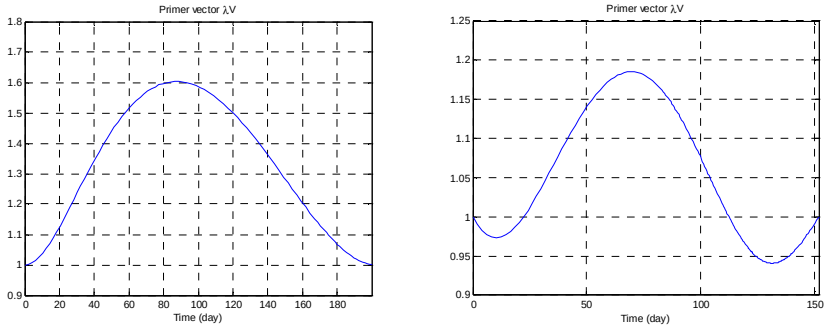

Figure 7. Non optimal trajectories

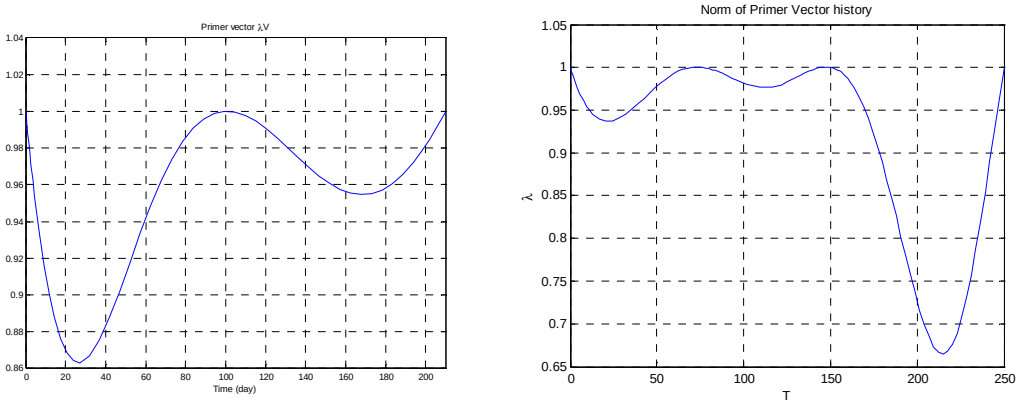

Figure 8. Optimal trajectories

Using the 4 conditions provided in 2.2.2, the primer vector theory provides a visual assessment of the optimality of a trajectory.

2.6 Applications

2.6.1 Earth – Mars direct transfer

Table 8.
Primer Vector, Earth Mars transfer

	NON OPTIMAL	OPTIMIZED
Departure	01/04/2001 12:00:00	
Arrival	28/10/2001 12:00:00	
Duration	210 days	
[Earth] -> [Mars]		
ΔV_0	3.30 km/s	2.73 km/s
DSM #1		T0+100.5days, 0.524 km/s, 1.23AU
RendezVous maneuver	**3.54 km/s**	**3.22 km/s**
Total ΔV	**6.843 km/s**	**6.475 km/s**

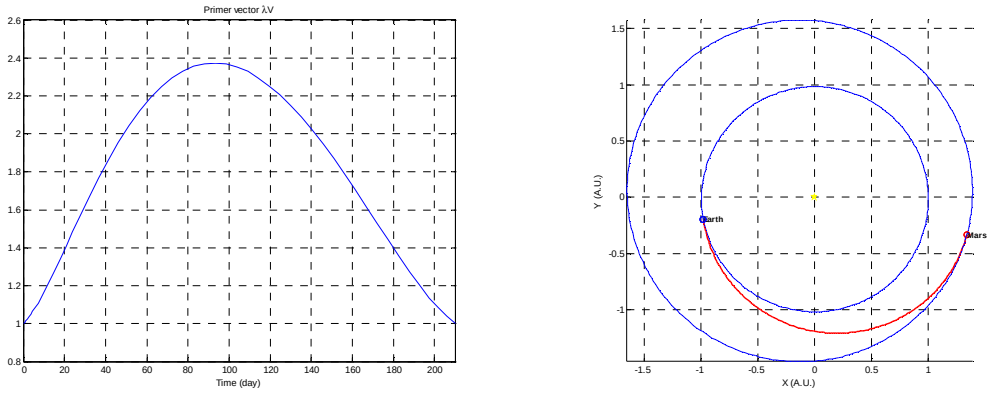

Figure 9. Non optimal Earth Mars transfer

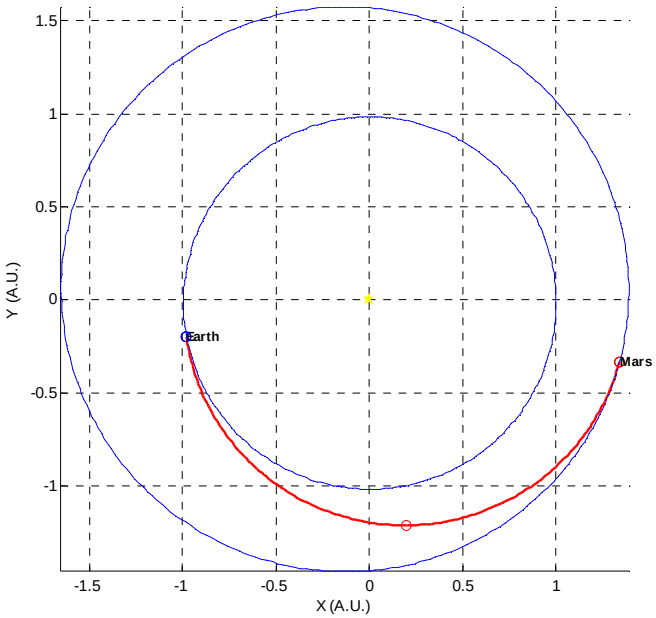

Figure 10. EM optimal 1-impulse trajectory

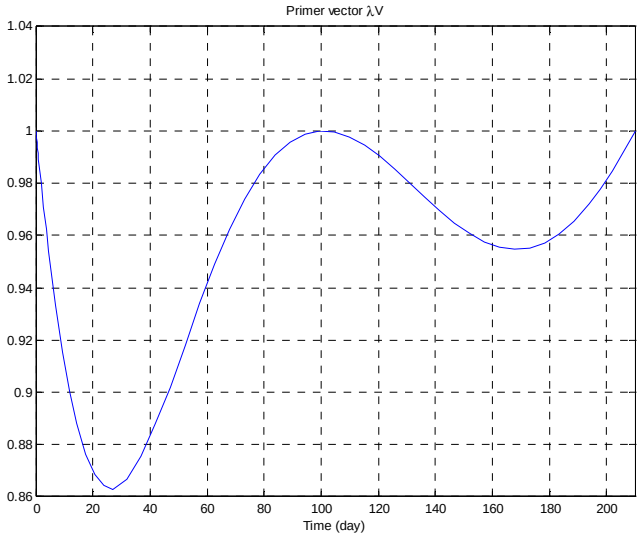

Figure 11. Direct primer optimal Earth-Mars trajectory

The optimization process had one impulse and managed to reduce both the initial and the final impulsive manoeuvres.

2.6.2 Earth – Venus

Table 9. Primer Vector, Earth - Venus transfer

	NON OPTIMAL	OPTIMIZED
Departure	31/05/2007	
Arrival	05/02/2008	
Duration	250 days	

[Earth] -> [Venus]		
T	250.0 days (JD: 2454251.500)	
ΔV_0	28.61 km/s	2.66 km/s
DSM #1	-	T0+75.6 days, 0.356 km/s, 0.87AU
DSM #2	-	T0+145.0 days, 2.832 km/s, 0.72AU
RendezVous maneuver	**37.520 km/s**	**0.011 km/s**
Total ΔV	**66.129 km/s**	**5.861 km/s**

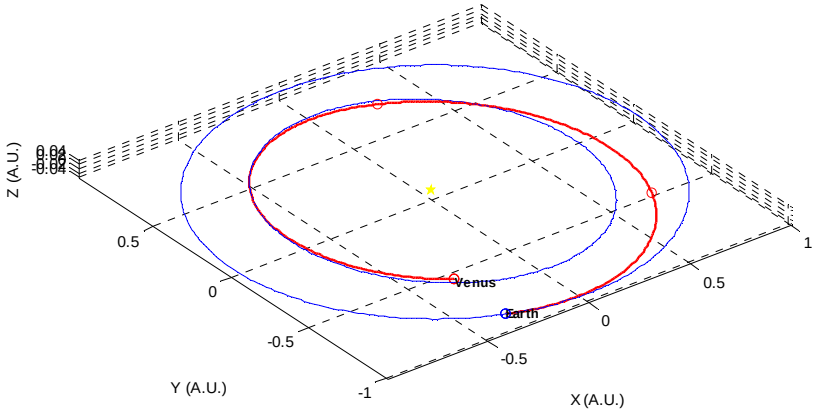

Figure 12. EV optimal 2-impulse trajectory

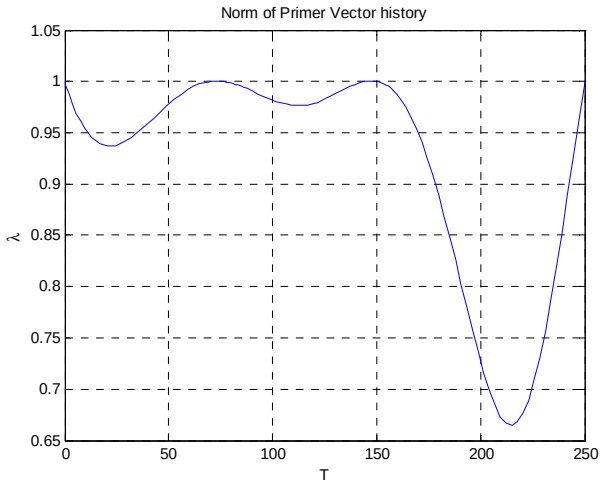

Figure 13. EV primer optimal trajectory

This example is particularly interesting as the reference case is a highly energetic trajectory. Actually the date has been chosen such that the trajectory is almost perpendicular to the ecliptic. Adding impulses typically bring back the trajectory close to the ecliptic. The reduction of the cost is here quite significant.
This example also emphasizes the necessity to need sometimes more than one impulse.

2.6.3 Earth – Mars global optimization

We propose to globally optimize a simple EM (Earth-Mars) direct transfer, with rendezvous conditions.
The purpose is to illustrate the efficiency of the numerical method, as well as demonstrating that solution considering more than one DSM can be helpful.

Table 10. Search Box

	Lower bound	Upper bound	Step
Launch date (MJD2000)	2557	2957	10 days
ToF (days)	100	500	10

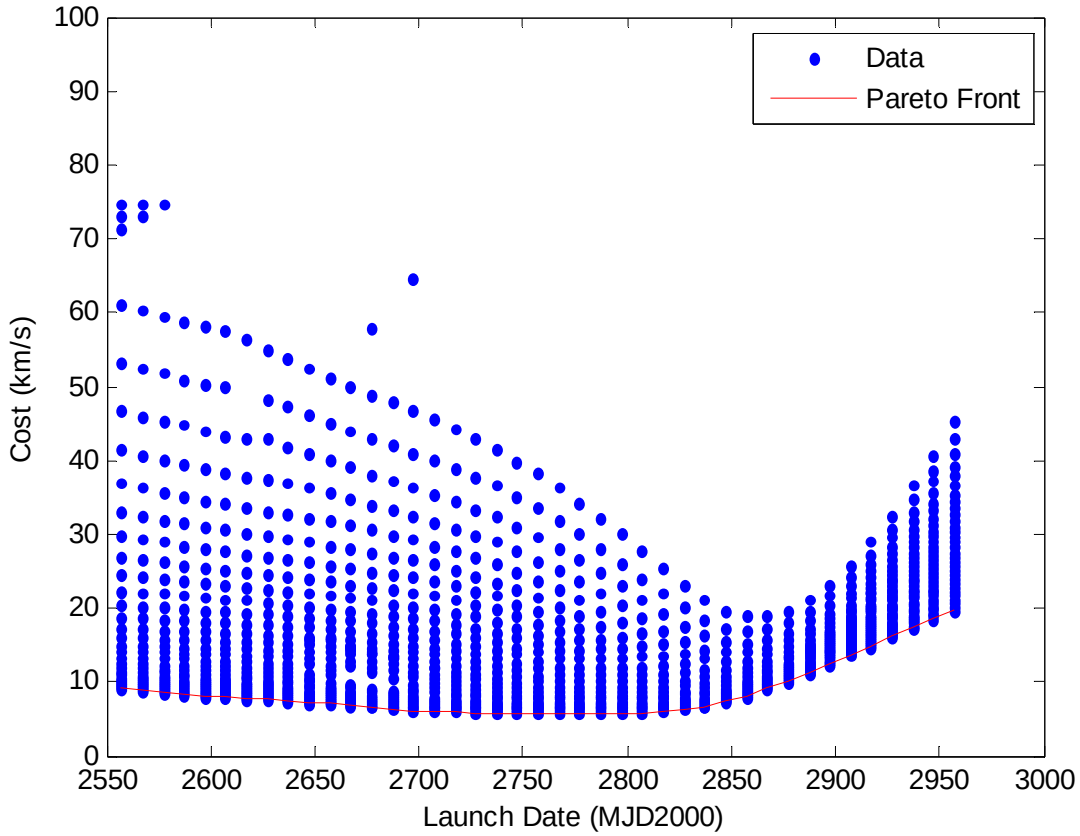

Figure 14. Global optimization of an EM transfer

Because we search in a grid, instead of randomly evaluating point, the points on Figure 14 seem actually ordered. There is however little chance we miss good points in this search space according to the smooth shape of the Pareto front.

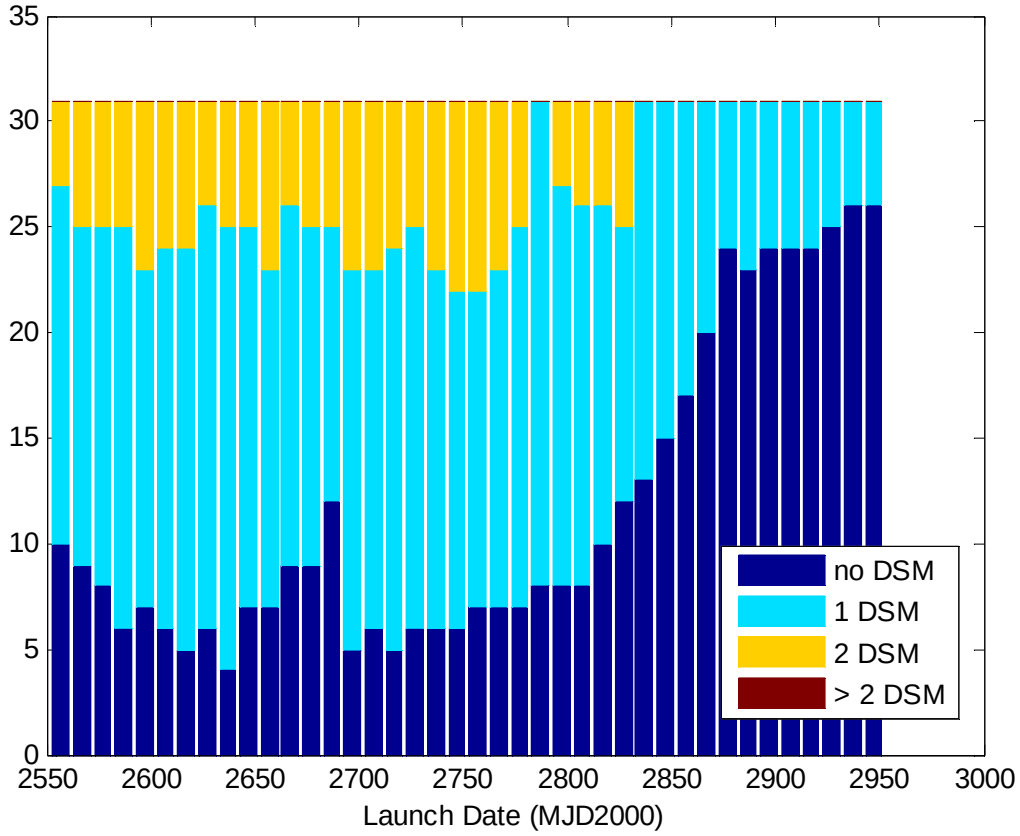

Figure 15. Distribution of DSM solutions for an EM transfer.

Figure 15 shows the distribution of the solution. We investigate the number of DSM for each point of Table 10. As one can notice, most of the time the cost can be reduced with DSM. There are few 2 DSM solutions, and no solution with more than 2 DSM. Indeed, 2 DSM solutions generally appear to high inclination transfer or when the transfer is closed to the π-singularity of the Lambert's problem. For example, we can expect solutions with more than 2 DSM for direct EY transfers.

2.7 Conclusions

We introduce the primer vector theory. The minimization of the characteristic velocity of a leg can be done through the use of a local optimization solver. The number of DSM is free and optimally found be the algorithm.

Beside the fact that the Primer vector theory allows the use of multiple DSM on single leg, it indicates before all, if we need to place DSM. This avoids placing unpromising DSM on the trajectory. This point is of great importance, because without the primer vector theory one is able to find an optimum for a given and fixed number of impulses. However, this optimum, although it verifies the necessary and eventually sufficient conditions of optimality, as little

chance to be the global optimum if this one needs more impulses. So far, major algorithms and code seek optimal trajectories with a constraint on the number of impulses.
Thus as stated earlier, the approach we propose is local. However this approach is still valid for global optimization as long as we are capable of finding the basin of attraction of the global optimum. It permits to find the global optimum as its formulation does not make any constraint on the number of impulses. Indeed, direct approach may be sub-optimal, whereas our indirect approach could not.

3 Primer Optimal MGA trajectories

3.1 Solution method

We can tackle the MGADSM problem with the primer vector theory. The usual approach is to compute the primer vector straight from t_0 to t_f, using the boundary condition at the swing-by. As for the simple transfer case, the maximum of λ above 1 determine the impulse to add.
This method may be attractive since it uses the method and algorithms introduced beforehand. However, one should notice that for multiple gravity assist trajectory, the global Two Point Boundary Value Problem (TPBVP) might become very sensitive.

The method followed here, performs trajectory decomposition and breaks the original trajectory at points of swing-by into separate legs. Subsequently, it optimizes each legs independently, using the primer vector theory, and with appropriate boundary conditions. These boundary conditions allow to communicate between the sub problems.
This method follows 2 steps:

- formulation of sub problems of lesser size than the initial problem (= decomposition)
- set up of an exchange process between the sub problem in order to comply with the initial problem (= coordination)

Using the optimization problem defined in 2.2, we extend the primer vector theory to multi gravity assist trajectories. In particular, we study the condition of optimality at the swing-by, on the primer vector. The conditions of optimality at the swing-by [16] have rarely been discussed.
The purpose is to get the optimum of the initial problem. The trajectory decomposition permits to remove the sensibility of the problem, and allows solving simpler sub problems.

3.2 Primer vector at Swing-By

To compute the primer vector history on the whole trajectory, 2 approaches may be followed.

- We can consider the free swing-by case. The trajectory contains only DSM between the swing-by. In this case, the primer vector is computed in a whole and optimization is done following the same technique as for the simple leg transfer. The drawback of this approach is the sensitivity of the trajectory when computing the primer vector for a TPBVP.
- We can consider powered swing-by. In this case, we decompose the whole trajectory in order to have legs that start and end with an impulse, and we can apply the same technique as for the simple leg transfer. In addition, we should coordinate the different leg optimisation to get the optimal trajectory.

As for the direct transfer case, we need sufficient boundary conditions to evaluate the primer vector history. The swing-by constraint introduces new conditions on the primer vector.

3.2.1 Swing-by and sphere of influence

To study the influence of a swing-by over the primer vector, we initially consider the sphere of influence and proceed in 3 steps. We study the primer when entering the sphere of influence, then the traversing of the sphere and finally exiting the sphere of influence.
For each of this step, we make a change of coordinate due to the different dynamics, since the central body switches from the Sun to the Planet and vice versa.

Following the approach of [9][10], we note the incoming and outgoing velocities at the sphere of influence:

$$\mathbf{V}_{in}^{+} = \mathbf{V}_{in}^{-} + \mathbf{V}_{pl}(t_{in}) \text{ and } \mathbf{V}_{out}^{-} = \mathbf{V}_{out}^{+} - \mathbf{V}_{pl}(t_{out}) \tag{3.1}$$

This transformation takes into account the change of coordinate and the planet velocity. The planet velocity should be evaluated for both the date of input and output in the Sphere of Influence.

Also at the crossing, the continuity of the Hamiltonian gives:

$$\boldsymbol{\lambda}_{\mathbf{V}}^{+T}\delta\mathbf{V}^{+} + \boldsymbol{\lambda}_{\mathbf{R}}^{+T}\delta\mathbf{R}^{+} = \boldsymbol{\lambda}_{\mathbf{V}}^{-T}\delta\mathbf{V}^{-} + \boldsymbol{\lambda}_{\mathbf{R}}^{-T}\delta\mathbf{R}^{-} \tag{3.2}$$

The case when exiting the sphere of influence is identical except that we must exchange the indices.

We then get the following relationship between the incoming and the outgoing co-state vectors:

$$\boldsymbol{\Lambda}^{+} = \begin{pmatrix} \boldsymbol{\lambda}_{\mathbf{R}} \\ \boldsymbol{\lambda}_{\mathbf{V}} \end{pmatrix} = \begin{pmatrix} I & B \\ 0 & I \end{pmatrix} \boldsymbol{\Lambda}^{-} \tag{3.3}$$

With:

$$\mathbf{B}_{in} = \frac{\mathbf{R}}{\mathbf{R}^{T}\mathbf{V}_{in}} \frac{d}{dt}\left(\mathbf{V}_{in}^{+} - \mathbf{V}_{in}^{-} - \mathbf{V}_{pl}(t_{in})\right) \tag{3.4}$$

If we leave the sphere of influence, or we enter the sphere of influence:

$$\mathbf{B}_{out} = \frac{\mathbf{R}}{\mathbf{R}^{T}\mathbf{V}_{out}} \frac{d}{dt}\left(\mathbf{V}_{out}^{+} - \mathbf{V}_{out}^{-} + \mathbf{V}_{pl}(t_{out})\right) \tag{3.5}$$

See [10] for more details on (3.3).

Now even though a swing-by doesn't last long, we should compute the trajectory in the Sphere of Influence. With the transition matrix $S = \Phi(t_{in}, t_{out})$ computed in the planet centered dynamics from t_{in} to t_{out} we have:

$$\boldsymbol{\Lambda}_{in}^{+} = S\boldsymbol{\Lambda}_{out}^{-} \tag{3.6}$$

If the swing-by were powered, the impulse would make the reation simpler. There would not be a explicit relation between $\mathbf{\Lambda}_{in}^{+}$ and $\mathbf{\Lambda}_{out}^{-}$.

We deduce a relation linking the primer vector before and after the swing-by, considering the real influence of the planet:

$$\mathbf{\Lambda}_{in}^{-} = W\mathbf{\Lambda}_{out}^{+} \tag{3.7}$$

$$W = \begin{pmatrix} I & B_{in} \\ 0 & I \end{pmatrix} S \begin{pmatrix} I & B_{out} \\ 0 & I \end{pmatrix} \tag{3.8}$$

Equations (3.4), along with the Property 2.1 provide the following properties.

Property 3.1:
We have 3 conditions for a ballistic trajectory to be optimal at a swing-by:

- *the primer vector is continuous before, after and during a swing-by*
- *there is a discontinuity of the primer derivative when crossing the sphere of influence, due to a change of coordinate*
- *if the swing-by is free,* $\|\boldsymbol{\lambda}\| < 1$

These conditions, with the conditions on the primer vector for a planet to planet transfer to be optimal, allow constructing a primer optimal MGA DSM trajectory.

3.2.2 Boundary conditions for the patched conic approximation

We consider the patched conic approximation, with massless swing-by planets. Thus, there is a trajectory break where we have to patch 2 conics together. But patching the costate trajectories is less obvious as they do not define physical value. We define boundary conditions, which are a simplification of the result of section 3.2.1.

For the problem of minimization, with the objective function:

$$J = \sum_{i=1}^{N} \|\Delta \mathbf{V}_i\| \tag{3.9}$$

And the constraints for the swing-by:

$$\begin{aligned} \mathbf{R}^{-} &= \mathbf{R}^{+} = \mathbf{R} \\ \mathbf{V}_{\infty}^{+} &= Q(\beta)\mathbf{V}_{\infty}^{-} \\ \mathbf{V}^{+} &= \mathbf{V}_{pl} + \mathbf{V}_{\infty}^{+} \end{aligned} \tag{3.10}$$

We get the augmented value function:

$$I = J + \int_{t_0}^{t^-} \mathbf{\Lambda}^T \cdot F(\mathbf{x},t)dt + \int_{t^+}^{t_f} \mathbf{\Lambda}^T \cdot F(\mathbf{x},t)dt + \boldsymbol{\mu}^T\left(\mathbf{R}^{+} - \mathbf{R}^{-}\right) + \mathbf{v}^T\left(\mathbf{V}_{\infty}^{+} - \mathbf{Q}(\beta)\mathbf{V}_{\infty}^{-}\right) \tag{3.11}$$

With:

$$\mathbf{F}(\mathbf{x},t)=\begin{bmatrix}\mathbf{V}-\dfrac{d\mathbf{R}}{dt}\\ G(\mathbf{R})\mathbf{R}-\dfrac{d\mathbf{V}}{dt}\end{bmatrix}\text{ and }\boldsymbol{\Lambda}=\begin{bmatrix}\boldsymbol{\lambda}_R\\ \boldsymbol{\lambda}\end{bmatrix}$$

Note that we do not include the control in F, as it is already included in J. Consequently the Hamiltonians do not depend explicitly on the control.

Taking the differential of the value function *I*, we get:

$$\begin{aligned}dI = {} & dJ+\boldsymbol{\lambda}^T(t_f)d\mathbf{V}_f-\boldsymbol{\lambda}(t_0)d\mathbf{V}_0\\ & +\left(\boldsymbol{\mu}+\boldsymbol{\lambda}_R(t^+)\right)^T d\mathbf{R}^+-\left(\boldsymbol{\mu}+\boldsymbol{\lambda}_R(t^-)\right)^T d\mathbf{R}^-\\ & +\left(\mathbf{v}+\boldsymbol{\lambda}(t^-)\right)d\mathbf{V}_\infty^+-\left(\mathbf{v}^T\cdot\mathbf{Q}(\beta)+\boldsymbol{\lambda}(t^+)\right)^T d\mathbf{V}_\infty^-\\ & +\int_{t_0}^{t^-}\frac{d\left(\boldsymbol{\Lambda}^T\cdot\mathbf{F}(\mathbf{x},t)\right)}{d\mathbf{x}}d\mathbf{x}dt+\int_{t^+}^{t_f}\frac{d\left(\boldsymbol{\Lambda}^T\cdot\mathbf{F}(\mathbf{x},t)\right)}{d\mathbf{x}}d\mathbf{x}dt\end{aligned}\tag{3.12}$$

The necessary conditions for optimality ($dI=0$), permits to get the known results:

$$\boldsymbol{\lambda}(t_f)=\frac{\Delta\mathbf{V}_f}{\left\|\Delta\mathbf{V}_f\right\|}\text{ and }\boldsymbol{\lambda}(t_0)=\frac{\Delta\mathbf{V}_0}{\left\|\Delta\mathbf{V}_0\right\|}$$

$$\boldsymbol{\Lambda}^T\cdot\frac{d\mathbf{F}(\mathbf{x},t)}{d\mathbf{x}}=0$$

But also:

$$\begin{cases}\boldsymbol{\lambda}_R(t^+)=\boldsymbol{\lambda}_R(t^-)=\boldsymbol{\mu}\\ \boldsymbol{\lambda}(t^-)=\mathbf{v}\\ \boldsymbol{\lambda}(t^+)=\mathbf{v}^T\cdot\mathbf{Q}(\beta)\end{cases}\tag{3.13}$$

Those last conditions give the boundary conditions at the swing-by.
And:

$$\boldsymbol{\lambda}(t^+)=\frac{\mathbf{V}_\infty^+}{\left\|\mathbf{V}_\infty^-\right\|}\frac{\mathbf{V}_\infty^-}{\left\|\mathbf{V}_\infty^-\right\|}\boldsymbol{\lambda}(t^-)\tag{3.14}$$

For a non-powered swing-by, we have $\left\|\mathbf{V}_\infty^-\right\|=\left\|\mathbf{V}_\infty^+\right\|$, such that the primer vector is continuous in module. Different expression can be found in the literature according to the expression of the constraint used for the swing-by model. (see Glandorf[10], Konstantinov Fedotov Petukhov[11]).

These boundary conditions, however forbid us to use directly the transition matrix directly from t_0 to t_f. We must use the intermediate matrix:

$$W = \begin{pmatrix} I & 0 \\ 0 & \dfrac{\mathbf{V}_\infty^+}{\left\|\mathbf{V}_\infty^-\right\|} \dfrac{\mathbf{V}_\infty^-}{\left\|\mathbf{V}_\infty^-\right\|} \end{pmatrix} \tag{3.15}$$

The overall transition matrix, describing the MGADSM problem, is written:

$$\Phi(t_f, t_0) = \Phi(t_f, t_{GA}) \cdot W \cdot \Phi(t_{GA}, t_0) \tag{3.16}$$

To get the value of $\boldsymbol{\lambda}$ at $t_{GA}{}^+$ or $t_{GA}{}^-$, we use a transition matrix development:

$$\begin{aligned} &\left(I - \phi_{12}^{-1}\left(t_0, t_{GA}{}^-\right)\phi_{11}\left(t_0, t_{GA}{}^-\right)\phi_{11}\left(t_{GA}{}^+, t_f\right)\phi_{12}\left(t_f, t_{GA}{}^+\right)\right)\frac{d\boldsymbol{\lambda}}{dt}\left(t_{GA}{}^-\right) = \phi_{12}^{-1}\left(t_0, t^-\right)\left[\boldsymbol{\lambda}_0 - \phi_{11}\left(t_0, t_f\right)\boldsymbol{\lambda}_f\right] \\ &\boldsymbol{\lambda}\left(t_{GA}{}^+\right) = \phi_{11}^{-1}\left(t_f, t_{GA}{}^+\right)\left(\boldsymbol{\lambda}_f - \phi_{12}\left(t_f, t_{GA}{}^+\right)\frac{d\boldsymbol{\lambda}}{dt}\left(t_{GA}{}^+\right)\right) \end{aligned} \tag{3.17}$$

Where:

$$\boldsymbol{\lambda}_0 = \boldsymbol{\lambda}(t_0)$$

$$\boldsymbol{\lambda}_f = \boldsymbol{\lambda}(t_f)$$

And:

$$\frac{d\boldsymbol{\lambda}}{dt}\left(t_{GA}{}^-\right) = \frac{d\boldsymbol{\lambda}}{dt}\left(t_{GA}{}^+\right)$$

The properties 3.1 remain valid in the patched conic approximation.

3.3 Resolution of MGA trajectory

3.3.1 Interaction Prediction Principle

In the most general case, when *J* is additive we can write:

$$J(\mathbf{u}) = \sum_i J_i(\mathbf{u}_i)$$

Then we simply have to solve:

$$\min_{\mathbf{u}_i}\left(J_i(\mathbf{u}_i)\right) \text{ for i=1..n}$$

Under the constraints:

$$\psi_{ii} = \vartheta_i - c_{\psi i}$$
$$c_{\psi i} = \sum_{j \neq i} \psi_{ji}$$

Where ϑ_i is the constraint for the sub problem *i*, $c_{\psi i}$ is the complementary part provided by the other sub problems. The constraints are what we can call essential constraints, since they are necessary to communicate between the sub problems. Each sub problems has a responsibility in the global problem resolution.

The calculus of variation gives the expression of the Lagrangian for the global problem:

$$L(\mathbf{u}, c_\psi, c_p, \mu) = \sum_{i=1}^{N} \left(J_i(\mathbf{u}_i) + \mu_i \left(\psi_{ii} - \vartheta_i + c_{\psi i} \right) + c_{pi} \left(c_{\psi i} - \sum_{j \neq i} \psi_{ji} \right) \right)$$

The necessary conditions of optimality give an update formula for the coordination parameters:

$$\frac{\partial L}{\partial c_{\psi i}} = \mu_i + c_{pi} = 0$$

$$\frac{\partial L}{\partial c_{pi}} = c_{\psi i} - \sum_{j \neq i} \psi_{ij}(u) = 0$$

Applying this method to our problem gives sub-problems where we simply have to solve direct transfers.
Instead of the fixed point algorithm, one can use a more appropriate modified Uzawa algorithm or the Arrow – Hurwicz algorithm.

Arrow-Hurwicz Algorithm
Consider the minimisation problem:

$$\min_{c(x)=0} f(x)$$

From an initial point $x^0 \in R^n, \lambda^0 \in R^m$, *and* $\varepsilon, \alpha \in R^+$. *Consider the projection* $p(\lambda)$ *on* R^+. *We iterate:*

$$x^{k+1} = x^k - \varepsilon \left(\nabla f(x^k) + \frac{\partial c}{\partial x}(x^k) \lambda^k \right)$$
$$\lambda^{k+1} = p\left(\lambda^k + \alpha c(x^k) \right)$$

Thus to find the saddle point, without constraints, we use:

$$c_\psi{}^{k+1} = c_\psi{}^{k} - \varepsilon_\psi \frac{\partial L}{\partial c_\psi}$$
$$c_p{}^{k+1} = c_p{}^{k} - \varepsilon_\psi \frac{\partial L}{\partial c_p}$$

Where ε and η must be considered as small positive scalar. We can make them vary through the iterations.

However, to work well this method supposes the existence of a saddle point that would permit to minimize the primal problem and maximize the dual problem in indifferent order (min-max or max-min).
In [12][13], the authors present other efficient approach as improvement of the Arrow – Hurwicz algorithm and the use of the appropriate iterate in the update formulas.
Practically, to improve convergence, we add a local solver which solves the complete problem using the results of the decomposition steps.

3.3.2 Application to MGADSM space trajectory problems

3.3.2.1 General constraints and hypothesis

Each body to body transfer is considered as a sub problem. We use here non powered swing-bys, but impulses are allowed immediately after the swing-by. The constraints on the state represent the conditions at the swing by. According to the patched conic approximation, with a massless planet, the position is continuous and equal to the heliocentric planet position. The swing-by is not powered such that the constraint only accounts for the energetic conservation and the feasible swing-by altitude.

Noting that we are not actually interested by the plane of rotation of the swing-by defined by η, we have simply:

$$\boldsymbol{\psi}(t_i) = \begin{bmatrix} \mathbf{r}(t_i^+) - \mathbf{r}_\otimes(t_i) \\ \mathbf{r}(t_i^-) - \mathbf{r}_\otimes(t_i) \\ \left\|\mathbf{V}_\infty^-\right\| - \left\|\mathbf{V}_\infty^+\right\| \\ \dfrac{\mathbf{V}_\infty^{-T}\mathbf{V}_\infty^+}{\left\|\mathbf{V}_\infty^-\right\|^2} - \cos\left(\beta\left(r_p, \left\|\mathbf{V}_\infty^-\right\|\right)\right) \end{bmatrix} \tag{3.18}$$

The function $\beta\left(r_p, \left\|\mathbf{V}_\infty^-\right\|\right)$ gives the angle of deviation for a given radius of periapsis r_p and a given incoming relative velocity $\left\|\mathbf{V}_\infty^-\right\|$. The variable r_p is an unknown of the general problem. The constraint on the incoming and outgoing relative velocity can also be expressed using the rotation matrix $Q\left(r_p, V_\infty, \eta\right)$, however this relation would introduce an additional variable η which is of no interest here.

3.3.2.2 Control

For a body to body transfer, the leg is described by the initial and final positions, and the *m* DSM description. According to chapter 1.1, a DSM is described by 4 variables which can be either position or the ΔV velocity vector and the date of the impulse.

The decision vector used is:

$$\mathbf{z} = \left[t_1, \mathbf{r}_1, ,..., t_n, \mathbf{r}_n, r_p\right]$$

The date of the DSM are sorted $t_0 < t_1 < ... < t_i < ... < t_n < t_f$.

Describing the impulses with their positions in space is appealing as we could use a Lambert's problem solver. The Lambert's problems are restricted to be less than a revolution to ensure the existence, uniqueness and reliability of the solution found. This restriction does not limit the number of DSM-leg revolution, and encourage the solver to add revolutions when increasing the number of DSM. Plus, it model simplifies the constraints Eq. (3.18).

Remark:
Another model such as the date-velocity model, needs to include the final position constraint which provides an additional Lagrange multiplier. This additional Lagrange multiplier however, provides interesting information on the optimality of the current trajectory when the primer vector at the one of the end cannot be evaluated properly. This description is better and more general for multiple revolution transfers as it does not need to specify the number of revolution. The major drawback is the evaluation of the derivatives.

In this paper only the time-position approach will be considered in the following developments.

3.3.2.3 Multi gravity assist formulation

Suppose we are solving a multi DSM transfer with *n* phases, and M_i DSM for the ith phase. The launch date t_0, the arrival date t_f and the planet encounter date t_i define the scenario. We then write a new Lagrangian function for the optimal control problem:

$$\mathcal{L}\left(\mathbf{z}, \mathbf{r}_p, \mathbf{v}\right) = \sum_{i=1}^{n} J_i\left(\mathbf{z}\right) + \sum_{i=1}^{n-1} \mathbf{v}_i{}^T \begin{bmatrix} \left\|\mathbf{V}_{\infty,i}^-\right\| - \left\|\mathbf{V}_{\infty,i+1}^+\right\| \\ \dfrac{\mathbf{V}_{\infty,i}^- \cdot \mathbf{V}_{\infty,i+1}^+}{\left\|\mathbf{V}_{\infty,i}^-\right\|^2} - \cos\left(\beta\left(r_{pi}, \left\|\mathbf{V}_{\infty,i}^-\right\|\right)\right) \end{bmatrix} \tag{3.19}$$

The value function $J_i\left(\mathbf{z}\right) = \sum_{j=1}^{M_i} \left\|\Delta\mathbf{V}_{j,i}\right\|$ is the cost of each phase and the impulse $\Delta\mathbf{V}_{j,i}$ stands for the jth impulse of the ith phase. The 2x1 vectors $\mathbf{v}_i$ are the constant Lagrange variable associated to the swing by constraint. As illustrated on Fig. 1, the decomposition is done at each intermediate body (where a swing-by occurs).

$$\mathbf{z} = \left[\mathbf{z}_1, ..., \mathbf{z}_k, ..., \mathbf{z}_n\right]$$

Where $\mathbf{z}_k$ is the decision vector of the k[th] sub-problem or phase. We consider *n* independent sub-problems.

To stay consistent with the optimality of the overall problem, we create a coordination variable for each missing information. Thus, for the k[th] sub problem, a coordination variable $\mathbf{c}_{v,k}$ is associated to Lagrange variables corresponding to the swing-by constraint, and coordination variables $\mathbf{c}_{\infty,k}$ are associated to the incoming or outgoing hyperbolic excess velocity. When we decompose and isolate a leg, all the information needed to compute an optimum of the original problem is given by the coordination variables.

The sub problems to solve are described by the new Lagrangian merit functions (see Fig. 1 for notation description):

$$\begin{aligned}\mathcal{L}_1\left(\mathbf{z}_1, r_{p,1}, \mathbf{c}_{\infty,1}\right) = \left\|\Delta\mathbf{V}_0\right\| + \sum_{i=1}^{M_1}\left\|\Delta\mathbf{V}_{i,1}\right\| + \\ + \nu_1{}^T\begin{bmatrix}\left\|\mathbf{V}_{\infty,1}^-\right\| - \left\|\mathbf{c}_{\infty,1}\right\| \\ \dfrac{\mathbf{V}_{\infty,1}^-\mathbf{c}_{\infty,1}}{\left\|\mathbf{v}_{\infty,1}^-\right\|^2} - \cos\left(\beta\left(r_{p,1}, \left\|\mathbf{V}_{\infty,1}^-\right\|\right)\right)\end{bmatrix}\end{aligned} \tag{3.20}$$

$$\begin{aligned}\mathcal{L}_n\left(\mathbf{z}_n, r_{p,n-1}, \mathbf{c}_v, \mathbf{c}_{\infty,n}\right) = \sum_{i=1}^{M_n}\left\|\Delta V_{i,n}\right\| + \left\|\Delta\mathbf{V}_f\right\| + ... \\ + \mathbf{c}_{v,n}{}^T\begin{bmatrix}\left\|\mathbf{c}_{\infty,n}\right\| - \left\|\mathbf{V}_{\infty,n}^+\right\| \\ \dfrac{\mathbf{c}_{\infty,n}\mathbf{V}_{\infty,n}^+}{\left\|\mathbf{c}_{\infty,n}\right\|^2} - \cos\left(\beta\left(r_{p,n-1}, \left\|\mathbf{c}_{\infty,n}\right\|\right)\right)\end{bmatrix}\end{aligned} \tag{3.21}$$

$$\begin{aligned}\mathcal{L}_k\left(\mathbf{z}_k, r_{p,k-1}, \mathbf{c}_{v,k}, \mathbf{c}_{\infty,k}, \mathbf{c}_{\infty,k+1}\right) = \sum_{i=1}^{M_k}\left\|\Delta\mathbf{V}_{i,k}\right\| + \\ + \nu_k{}^T\begin{bmatrix}\left\|\mathbf{V}_{\infty,k}^-\right\| - \left\|\mathbf{c}_{\infty,k+1}\right\| \\ \dfrac{\mathbf{V}_{\infty,k}^-\mathbf{c}_{\infty,k+1}}{\left\|\mathbf{V}_{\infty,k}^-\right\|^2} - \cos\left(\beta\left(r_p, \left\|\mathbf{V}_{\infty,k}^-\right\|\right)\right)\end{bmatrix} \\ + \mathbf{c}_{v,k}{}^T\begin{bmatrix}\left\|\mathbf{c}_{\infty,k}\right\| - \left\|\mathbf{V}_{\infty,k}^+\right\| \\ \dfrac{\mathbf{c}_{\infty,k}\mathbf{V}_{\infty,k}^+}{\left\|\mathbf{c}_{\infty,k+1}\right\|^2} - \cos\left(\beta\left(r_{p,k-1}, \left\|\mathbf{c}_{\infty,k+1}\right\|\right)\right)\end{bmatrix}\end{aligned} \tag{3.22}$$

These expressions stand respectively for the initial phase, the final phase, and the intermediate phases $k \in \{2,...,n-1\}$. As one can notice, the equations (3.21) and (3.22) include coordination parameters which stand for the coupling relations defined by Eq. (3.18). Because of these extended functions the optimal solutions of Eqs. (3.20 – 3.22) are not the solutions which are optimal with respect to the sum of impulse over the leg but they are optimal solutions for the overall problem defined by Eq. (3.19). At convergence of the algorithm, if one sum up the equations (3.20 – 3.22) it would result in the general MGADSM function cost with intermediate swing by constraints.

$$\mathcal{L}\left(\mathbf{z}^*, \mathbf{r}_p, \mathbf{v}\right) \equiv \mathcal{L}_1\left(\mathbf{z}_1^*, r_{p,k-1}, \mathbf{c}_{\infty,1}\right) + \mathcal{L}_n\left(\mathbf{z}_n^*, r_{p,n-1}, \mathbf{c}_{v,n}, \mathbf{c}_{\infty,n}\right) + \sum_{k=2}^{k=n-1} \mathcal{L}_k\left(\mathbf{z}_k^*, r_{p,k-1}, \mathbf{c}_{v,k}, \mathbf{c}_{\infty,k}, \mathbf{c}_{\infty,k+1}\right)$$

3.3.2.4 Boundary conditions

The primer vector module history is provided by the same boundary values on the primer vector. At the initial time of the leg this value is provided by the coordination variable or the initial impulse for the first leg. At the final time of the leg the boundary value on the primer vector is given by the Lagrange variable of the final constraint.

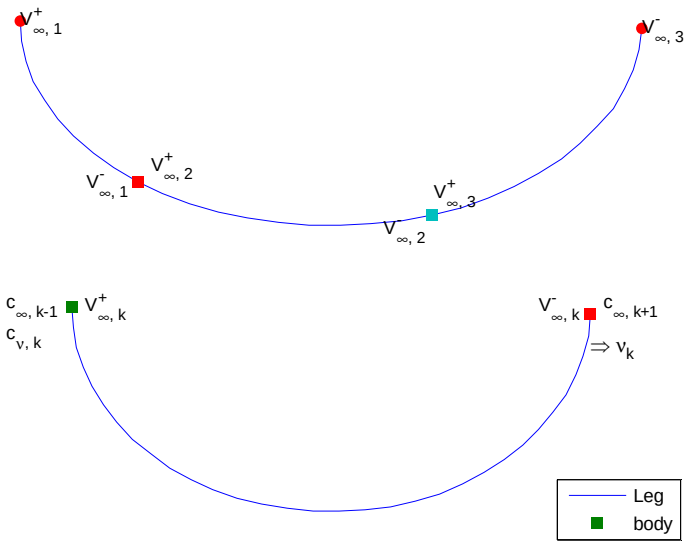

Figure 16. Illustration of the Decomposition step

Comparing the OCP with the POP, for the initial sub problem at $t = t_0$ we have:

$$\boldsymbol{\lambda}_V\left(t_0\right) = \frac{\Delta\mathbf{V}_0}{\left\|\Delta\mathbf{V}_0\right\|} \qquad (3.23)$$

$$\boldsymbol{\lambda}_V\left(t_1^-\right) = -\nu_1 \frac{\mathbf{V}_{\infty,0}^-}{\left\|\mathbf{V}_{\infty,0}^-\right\|}$$

For the final sub problem we have:

$$\boldsymbol{\lambda}_V\left(t_n^+\right) = c_\nu \frac{\mathbf{V}_{\infty,n}^+}{\left\|\mathbf{V}_{\infty,n}^+\right\|} \qquad (3.24)$$

$$\boldsymbol{\lambda}_V\left(t_f\right)=\frac{\Delta\mathbf{V}_f}{\left\|\Delta\mathbf{V}_f\right\|}$$

The boundary conditions necessary to initialize the primer vector come from the necessary conditions of optimality for the intermediate sub problems. Thus:

$$\begin{aligned}\boldsymbol{\lambda}\left(t_k^{\ +}\right)&=-c_{v,k}\frac{\mathbf{V}_{\infty,k}^{\ -}}{\left\|\mathbf{V}_{\infty,k}^{\ -}\right\|}\\ \boldsymbol{\lambda}\left(t_{k+1}^{\ -}\right)&=\nu_k\frac{\mathbf{V}_{\infty,k}^{\ +}}{\left\|\mathbf{V}_{\infty,k}^{\ +}\right\|}\end{aligned}\tag{3.25}$$

3.3.2.5 Coordination step

After each iteration *i* of the algorithm (section D.I) the coordination step updates the coordination variables. The coordination formulas are provided by:

$$\begin{cases}\mathbf{c}_{v,k}^{i+1}=\left(1-\varepsilon_v\right)\mathbf{c}_{v,k}^{i}+\varepsilon_v\mathbf{v}_k\\ \mathbf{c}_{\infty,k}^{i+1}=\left(1-\varepsilon_\psi\right)\mathbf{c}_{\infty,k}^{i}+\varepsilon_\psi\mathbf{V}_{\infty,k}^{+}\\ \mathbf{c}_{\infty,k+1}^{i+1}=\left(1-\varepsilon_\psi\right)\mathbf{c}_{\infty,k+1}^{i}+\varepsilon_\psi\mathbf{V}_{\infty,k}^{-}\end{cases}\tag{3.26}$$

The coordination variables $\left\{\mathbf{c}_{v,k},\mathbf{c}_{\infty,k}\mathbf{c}_{\infty,k+1}\right\}$ along with $\left\{\mathbf{v}_k,\mathbf{V}_{\infty,k}^{-},\mathbf{V}_{\infty,k+1}^{+}\right\}$ allow respecting the swing by constraint and force the sub-problems solutions toward the overall problem solution.

Following Lawden primer vector theory, an important point should be made for the primer vector optimal MGA-DSM trajectory. For a MGA-DSM trajectory to be optimal, we must have $\left\|\mathbf{v}\right\|\leq 1$. Indeed, if $\left\|\mathbf{v}\right\|$ exceed 1, according to the equations (3.23, 3.24, 3.25), the primer vector also exceed one. As the primer vector histories for each sub problem can be patched together according to Eqs. (3.20, 3.21, 3.22), the patched primer vector history couldn't be optimal for the complete problem.

Interestingly, we can note that adding impulses permits to lower the Lagrange variable module $\left\|\mathbf{v}\right\|$. According to the Hamilton-Jacobi theory [34], Lagrange variables represent the sensitivity of the constraint with respect to the decision vector. Thus, the more impulses we have, the more robust is the trajectory. This can also be interpreted considering that the final constraint relies on many intermediate impulses with small contributions, rather than on a single impulse with a high contribution.

3.3.2.6 Convergence

To improve the convergence of the program, we remove the angular deviation constraint on the velocity for the swing by in Eq. (3.19). We only keep the energetic conservation of swing-by. Once the energetic constraint is respected, we can further check for the swing-by angular deviation. We can re-optimize the solution with the minimum swing by altitude constraint.
As the primer vector theory predicts, we do not always need to insert deep space maneuvers on a leg. In this case, as the intermediate leg is the solution of a Lambert's problem, the constraints cannot always be satisfied. The initial and final hyperbolic excess velocity $\mathbf{V}_\infty^-$ and $\mathbf{V}_\infty^+$ are imposed by the Lambert solution and the departing and arrival planet velocities. It is not possible to get a Lagrange variable ν_k as it is required in Eqs. (3.23, 3.24, 3.25), but the final hyperbolic excess velocity constraint on that leg has to be satisfied to respect the free swing-by condition. In this case, the Lagrance variable ν_k is chosen free to minimize the Lagrangian which indirectly provides a non optimal leg as the primer vector module is likely to exceed unity at boundaries. We then considered two cases. When the constraints are satisfied, the Lagrange variable ν_k is free. Its value is chosen to be the one of the preceding iteration and kept unchanged until the next iteration. When the constraints are not satisfied, an intermediate impulse is added to reduce the cost. This issue is only a transient issue because the algorithm has not reached a steady state. When steady, constraints are satisfied.

3.4 Numerical Analysis

3.4.1 Algorithm

Using the decomposed Lagrangian, and the coordination variable update formulas, we can construct the following algorithm.

Table 11.
Algorithm

Step 0. Initialization of coordination variables.
Choose $\left\{\mathbf{c}_{v,k}^0, \mathbf{c}_{\infty,k}^0\right\}$ for all $k \in \{1,...,n\}$
Set $i = 0$

Step 1. Resolution of the *initial* problem with $\mathbf{c}_{\infty,1}^i$ to get $\mathbf{x}_1$.
Resolution of the *intermediate* problems *k* with $\left\{\mathbf{c}_{v,k}^i, \mathbf{c}_{\infty,k}^i, \mathbf{c}_{\infty,k+1}^i\right\}$ to get $\mathbf{x}_k$ for all $k \in \{1,...,n\}$.
Resolution of the *final* problem with $\left\{\mathbf{c}_{v,n}^i, \mathbf{c}_{\infty,n}^i\right\}$ to get $\mathbf{x}_n$.

Step 2. Update coordination variables.
$i \leftarrow i+1$ and $\left\{\mathbf{c}_{v,k}^i, \mathbf{c}_{\infty,k}^i\right\}$.

Step 3. Resolution of global problem with $\mathbf{x} = [\mathbf{x}_1, \mathbf{x}_2, ..., \mathbf{x}_n]$ as initial guess and test of optimality. Go back to **Step 1** if it is has not converged.

Each sub problem can be solved with a SQP minimization solver. After each iterate we can try to solve the global problem because we should expect the sub problems solutions to be "near" or in the basin of attraction of the complete problem solution. It improves convergence of the fixed point algorithm and assures we are effectively near a minimum and not simply an extremum.

3.4.2 Analytical derivatives

As SQP solvers tend to converge faster and easier when gradients are provided, we calculated the gradient on the constraint on the hyperbolic excess velocity.
Unfortunately, we cannot express the objective function gradient with the primer vector and its derivative at the switching point. This come from the fact that in most cases the final boundary conditions are expressed with a Lagrange multiplier which is not necessarily available during the optimization, but also because of the expression of the final boundary, the objective function differential cannot be expressed as a scalar product between the gradient and the elemental deviation.

$$\frac{\partial\left\|\Delta\mathbf{V}_i\right\|}{\partial\mathbf{x}}=\frac{1}{\left\|\mathbf{V}\left(t_i^{+}\right)-\mathbf{V}\left(t_i^{-}\right)\right\|}\left(\frac{\partial\mathbf{V}\left(t_i^{+}\right)}{\partial\mathbf{x}}-\frac{\partial\mathbf{V}\left(t_i^{-}\right)}{\partial\mathbf{x}}\right),\left(\mathbf{V}\left(t_i^{+}\right)-\mathbf{V}\left(t_i^{-}\right)\right) \tag{3.27}$$

The constraints formulation expressed at each end of the legs permit to express the gradient of the constraint with the final leg velocity Jacobian matrix.

$$\frac{\partial\psi}{\partial\mathbf{x}}=\frac{1}{\left\|\mathbf{V}\left(t_f\right)-\mathbf{V}_{\otimes}\left(t_f\right)\right\|}\frac{\partial\mathbf{V}\left(t_f\right)}{\partial\mathbf{x}}\left(\mathbf{V}\left(t_f\right)-\mathbf{V}_{\otimes}\left(t_f\right)\right) \tag{3.28}$$

Note that (34) and (35) might mathematically present a singularity when the denominator tends toward 0. This case can only happen for the equation (34) and the initial and final impulses only. The primer vector theory should avoid cases where impulses are 0. Because of (27), (35) cannot become singular as in practice the hyperbolic excess velocity at swing-by should never reach 0.
The gradients are computed using the state transition matrix approach. The transition matrix is defined by the dynamical system similar to (7) and using $\mathbf{G}(t,\mathbf{r})$. We have then:

$$\begin{bmatrix}\delta\mathbf{r}(t_i)\\ \delta\mathbf{v}(t_i)\end{bmatrix}=\begin{bmatrix}\phi_1(t_i,t_f) & \phi_2(t_i,t_f)\\ \phi_3(t_i,t_f) & \phi_4(t_i,t_f)\end{bmatrix}\begin{bmatrix}\delta\mathbf{r}(t_f)\\ \delta\mathbf{v}(t_f)\end{bmatrix} \tag{3.29}$$

As we are solving a fixed time problem, the initial and final position perturbations are zero: $\delta\mathbf{r}_0=0$, $\delta\mathbf{r}_f=0$. A change in the final velocity induces a change in the position, velocity and date of the intermediate impulses $(\mathbf{r}_i,\mathbf{v}_i,t_i)$. The state transition matrix allows calculating the first order perturbation on the state and thus gives useful information for computing the derivatives. However, the state transition matrix can only describe perturbations between two instant where the spacecraft equation of motion are continuous.

Using the following general expressions:

$$\delta \mathbf{v}_i^{+} = \phi_2^{-1}(t_j, t_i)\left[\delta \mathbf{r}_j - \phi_1(t_j, t_i)\delta \mathbf{r}_i\right],\ j = i+1 \tag{3.30}$$

$$\delta \mathbf{v}_i^{-} = \phi_2^{-1}(t_k, t_i)\left[\delta \mathbf{r}_k - \phi_1(t_k, t_i)\delta \mathbf{r}_i\right],\ k = i-1 \tag{3.31}$$

and:

$$\delta \mathbf{v}_0 = \phi_2^{-1}(t_1, t_0)\delta \mathbf{r}_1 \tag{3.32}$$

$$\delta \mathbf{v}_f = \phi_2^{-1}(t_n, t_f)\delta \mathbf{r}_n \tag{3.33}$$

Indeed, because of the DSM model used and the Lambert's problem definition, an impulse $\Delta \mathbf{V}_i$ can be described only by the preceding and the next manoeuvre position and date $(t_i, \mathbf{r}_i)$.

We get the following derivatives:

$$\frac{\partial \mathbf{v}_i^{+}}{\partial \mathbf{r}_j} = \phi_2^{-1}(t_j, t_i), \quad \frac{\partial \mathbf{v}_i^{+}}{\partial \mathbf{r}_i} = -\phi_2^{-1}(t_j, t_i)\phi_1(t_j, t_i) \tag{3.34}$$

$$\frac{\partial \mathbf{v}_i^{+}}{\partial t_j} = \phi_2^{-1}(t_i, t_j)\mathbf{v}_j^{+}, \quad \frac{\partial \mathbf{v}_i^{+}}{\partial t_i} = -\phi_2^{-1}(t_j, t_i)\phi_1(t_j, t_i)\mathbf{v}_i^{+} \tag{3.35}$$

$$\frac{\partial \mathbf{v}_i^{-}}{\partial \mathbf{r}_j} = \phi_2^{-1}(t_j, t_i), \quad \frac{\partial \mathbf{v}_i^{-}}{\partial \mathbf{r}_i} = -\phi_2^{-1}(t_j, t_i)\phi_1(t_j, t_i) \tag{3.36}$$

$$\frac{\partial \mathbf{v}_i^{-}}{\partial t_j} = \phi_2^{-1}(t_j, t_i)\mathbf{v}_j^{-}, \quad \frac{\partial \mathbf{v}_i^{-}}{\partial t_i} = -\phi_2^{-1}(t_j, t_i)\phi_1(t_j, t_i)\mathbf{v}_i^{-} \tag{3.37}$$

3.5 Applications

3.5.1 Earth Venus Mars (EVM)

An Earth – Venus – Mars transfer is considered. The time of flight is fixed, as well as the launch date.

Table 12.
Optimal EVM MGA trajectory description

	NON OPTIMIZED	OPTIMIZED
Departure	08/06/2004 00:00:00	
Arrival	14/05/2005 00:00:00	
Duration	340 days	
[Earth] -> [Venus]		
T	165.0 days	(JD: 2453164.500)
ΔV_0	4.628 km/s	4.591 km/s
DSM	-	T0+96.08 days, ΔV = 68.7 m/s
Swing-By around Venus		
Date	20-Nov-2004	
Pericenter Altitude	7938.96 km	
Swing-by ΔV	3.84 km/s	-
Post swing-by ΔV	75.9 m/s	-
[**Venus] -> [Mars]**		
T	175.0 days	(JD: 2453329.500)
DSM	-	-
Rendezvous Manoeuvre	**6.142 km/**	**6.126 km/s**
Total ΔV	**10.847 km/s**	**10.786 km/s**

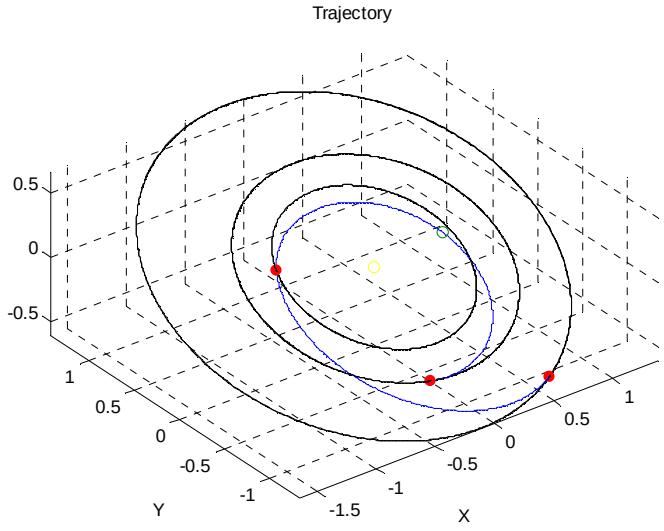

Figure 17. EVM optimized trajectory

This example shows a priori little gain in the overall cost. This is probably due to the reference case which is already a good solution to the no-DSM EVM transfer.
However, the reference case includes a post swing-by manoeuvre. The reference case is indeed more expensive. The EV swing-by permits to adjust correctly the swing-by conditions.

3.5.2 Earth Venus Earth Jupiter (EVEJ)

For this trajectory, we fix the departure and the different time of flight of each phase.

The MGA trajectory specifications are given on the table below:

Table 13.
EVEJ MGA trajectory. Primer Optimal comparison.

	NON OPTIMIZED	OPTIMIZED
Departure	18/09/2016 00:00:00	
Arrival	24/10/2021 00:00:00	
Duration	1862 days	
[Earth] -> [Venus]		
T	348.0 days	(JD: 2457649.500)
ΔV	4.59845 km/s	3.476 km/s
DSM #1	-	T0+95.64 days , ΔV = 0.008 m/s
DSM #2	-	T0+214.25 days, ΔV = 595.613 m/s
Swing-By around [Venus]		
Date	01-Sep-2017	
Arrival Vrel	8.184 km/s	
Pericenter Altitude	2220.86 km	
Swing-by ΔV	6.05 km/s	
Post swing-by ΔV	2.65 km/s	20.134 m/s
[Venus] -> [Earth]		
T	576.0 days	(JD: 2457997.500)
DSM #3	-	T0+475.64 days, ΔV = 0.001 m/s
DSM #4	-	T0+843.14 days, ΔV = 2.358 m/s
Swing-By around Earth		
Date	31-Mar-2019	
Arrival Vrel	12.362 km/s	
Pericenter Altitude	-277.45 km	
Swing-by ΔV	7.40 km/s	
Post swing-by ΔV	0.64 m/s	2.894 m/s
[Earth] -> [Jupiter]		
T	938.0 days	(JD: 2458573.500)
DSM	-	-
Rendezvous Manoeuvre	**6.19018 km/s**	**6.1902 m/s**
Total ΔV	**10.792 km/s**	**10.267 km/s**

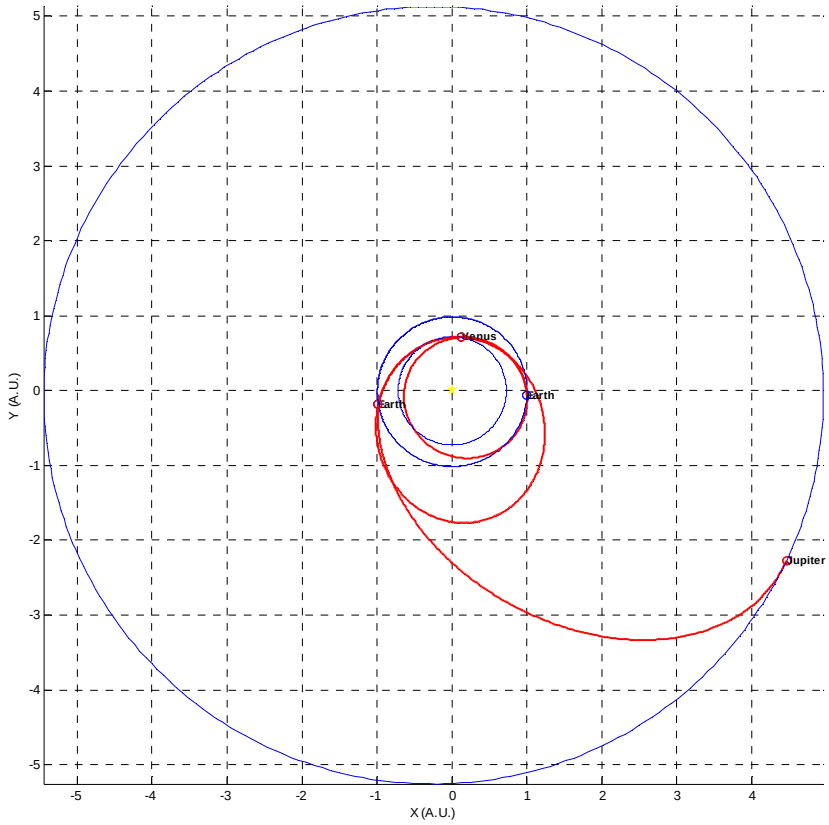

Figure 18. Non optimal EVEJ trajectory

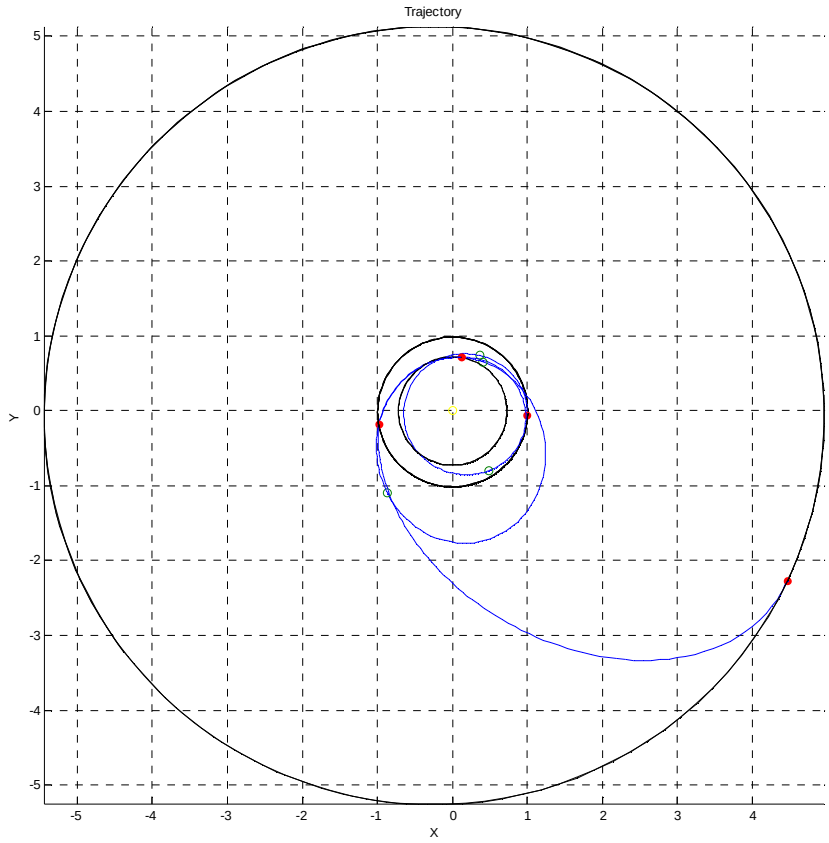

Figure 19. Optimal EVEJ trajectory

The gain is negligible (0.5 km/s), but the advantage of the optimised trajectory comes the reduced launch energy.
We notice that the optimal and non optimal trajectory match very closely.

3.5.3 Cassini Trajectory

The objective function to minimize is the sum of all the ΔV, plus the rendezvous manoeuvre and the initial hyperbolic excess velocity.
To illustrate the method, we use the phasing of known solutions [32], to check if we can further decrease the value function

Table 14. Search boxes

	T_0 (MJD 2000)	T_1 (days)	T_2 (days)	T_3 (days)	T_4 (days)	T_5 (days)
Case 1	-811.3	196.9	423.1	55.4	533.7	1573.8
Case 2	07/10/1997	197.334	425.171	56.8856	578.523	2067.98

Table 15. Search Space Domain

	Lb	Ub
T_{DSM} / ToF (days)	0.1	0.9
X_{DSM}, Y_{DSM} (A.U.)	-8.0	8.0
Z_{DSM} (A.U.)	-0.5	0.5

The best cost is reported to be 9.247 km/s (we computed 9.366 km/s) for the first case, and 9.06 km/s for the second case.

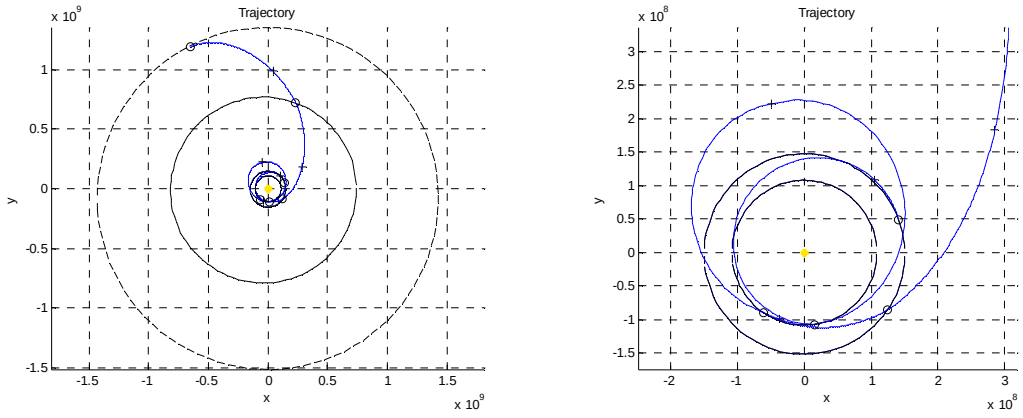

Figure 20. CASSINI trajectory (reference case 1)

Table 16.

	Solution 1 (T0+days)	ΔV (m/s)	Solution 2 (T0+days)	ΔV (m/s)
Launch ΔV_0	0	0	0	3906
DSM #1	29.85	3209	22.8	266.6
DSM #2	159.6	569.7	-	-
Venus Swingby	196.9		197.33	
DSM #3	423.17	425.5	438.3	415
DSM #4	-	-	-	-
Venus Swingby	620		622.51	
DSM #5	-	-	662.87	-
DSM #6	-	-	-	-
Earth Swingby	675.4	22.5	679.39	
DSM #7	-	-	730.80	-
DSM #8	-	-	-	-
Jupiter Swingby	1209.1	8.6	1257.91	
DSM #9	-	-	-	-
Rendezvous ΔV_f	2782.9	4709.7	3325.89	4289.2
TOTAL COST	**8.947 km/s**		**8.877 km/s**	

DSM of less than 1 m/s are not reported.

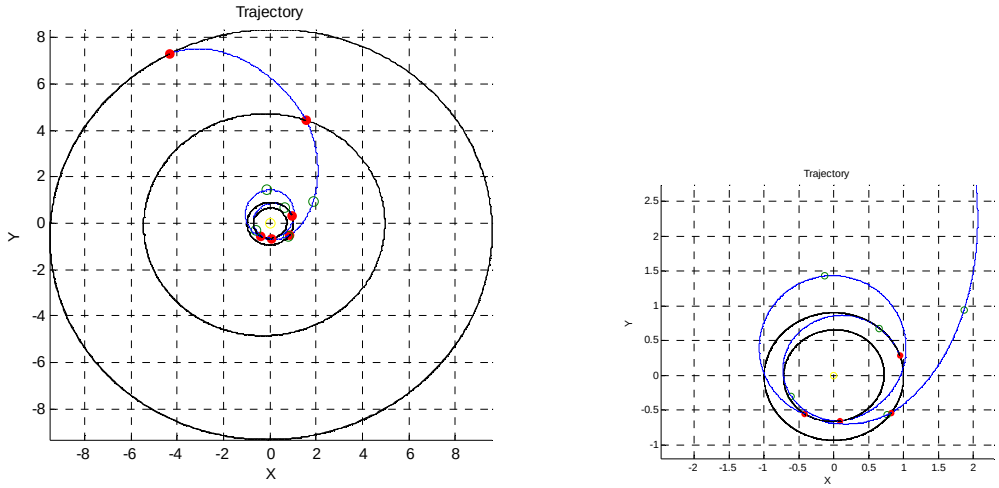

Figure 21. Cassini optimal MGADSM trajectory (optimized case 1)

This well reference example permits to show that the method is actually quite efficient. We manage to find about the same solution in the reference case 1.

3.6 Conclusions

We introduced the MGADSM problem. Our optimization approach permits the use of the results presented in the simple DSM case and the primer vector theory. Through a decomposition – coordination technique, the complete problem is solved by solving sub problem and finding their corresponding primer optimal trajectory for the given boundaries and constraints.

The method applied to known examples shows to be efficient as it permits to find the reported solution of the literature. Most importantly, the method use local optimization techniques and does not need any specification on the number of DSM. Consequently, the decision vector of the problem is only the date of departure and the dates of encounter as was done in the above example where these dates permit to find the good solution.
The method has however a slow (linear) convergence.

4 Automated approach for MGADSM trajectories

4.1 Partitioning method

4.1.1 Solution method description

The optimization method performs trajectory decomposition and breaks the original trajectory at points of swing-by into separate legs. We formulate sub-problems of lesser size than the initial problem which permits to remove the sensibility of the problem, and allow solving simpler sub problems. Subsequently, we optimize each sub-problem independently under specific boundary conditions which allow to communicate between the sub problems.
We are actually computing all possible extremals for each sub problems. Eventually, we compute a complete trajectory using those extremals and appropriate intermediate constraints.

4.1.2 Separable problems

In the most general case, let us suppose the minimization problem:

$$\min_{\mathbf{u}\in U} J(\mathbf{u})$$

Where U is in R^n.

In our problem, J is additive, such that we can write:

$$J(\mathbf{u}) = \sum_i J_i(\mathbf{u}_i) \tag{4.1}$$

Where $\mathbf{u} = [\mathbf{u}_1,...,\mathbf{u}_n]$.
Then we simply have to solve:

$$\min_{\mathbf{u}}\left(\sum_i J_i(\mathbf{u}_i)\right) \text{ for i=1..n}$$

Under the constraint of swing-by feasibility.

Unfortunately, the problem is not equivalent to solve: $\min_{\mathbf{u}_i}(J_i(\mathbf{u}_i))$ for each i if the problem is not separable.

Definition 4.1:
A nonlinear separable problem is a problem such that:

$$\min_{\mathbf{u}}\left(\sum_i J_i(\mathbf{u}_i)\right) = \bigcup_i \min_{\mathbf{u}_i} J_i(\mathbf{u}_i)$$

The minimization of a multivariable function is reduced to the simultaneous and independent minimization of multiple sub-problems.

The simplest example of separable problem is described by additive function.

4.1.3 Setting the partitioned problems

Duplication of variables

Consider the general minimisation problem:

$$\min_{\mathbf{X}\in\Re^M} J(\mathbf{X}) \tag{4.2}$$

Where J is a C^2 continuous function. We do not consider constraints.

Following, the number of phase or a natural decomposition, we duplicate each boundary variable and assign a copy to every process that needs the original. The decision vector $\mathbf{X}\in\Re^M$ turns into $\tilde{\mathbf{X}}\in\Re^K$. We divide $\tilde{\mathbf{X}}$ into n blocks $\{\mathbf{x}_1,...,\mathbf{x}_n\}$ where $\mathbf{x}_i\in\Re^N$, and $nN = K$ and $K = M + D$ where D is the number of duplicated variables. There are as much duplication as junction and junction variables.

Setting linking conditions

Now let's find $C\in M(\Re)_{D,K}$ such that we have an equality condition between the boundary duplicated variables and their respective originals:

$$C\begin{bmatrix}\mathbf{x}_1\\ ...\\ \mathbf{x}_n\end{bmatrix} = 0 \tag{4.3}$$

The constant matrix C is needed to account for the matching condition on the duplicated variables. C is a sparse matrix with one -1 and one 1 element on each line.

No information has been lost when duplicating and partitioning the problem.

Constructing complete solutions

The original problem can thus be re-written:

$$\min_{\mathbf{x}_i\in\Re^N} J_i(\mathbf{x}_i) \tag{4.4}$$

To construct complete solution we use the constraint on the duplicated variables:

$$C_i \begin{bmatrix} \mathbf{x}_i \\ \mathbf{x}_{i+1} \end{bmatrix} = 0 \tag{4.5}$$

This constraint ensures we can construct a complete trajectory.

4.2 GASP like formulation

4.2.1 Initial Problem

Let us recall the objective function, for a multi leg transfer:

$$J = \left\|\Delta\mathbf{V}_0\right\| + \left\|\Delta\mathbf{V}_f\right\| + \sum_{i=1}^{n} \left\|\Delta\mathbf{V}_{DSM(i)}\right\| \tag{4.6}$$

It is straight forward that in fact, each impulse can be rewritten as:

$$\begin{aligned} \Delta\mathbf{V}_0 &= \Delta\mathbf{V}_0\left(t_0, t_{DSM(1)}, r_{DSM(1)}\right) \\ \Delta\mathbf{V}_f &= \Delta\mathbf{V}_f\left(t_{DSM(n)}, t_f, r_{DSM(n)}\right) \\ \Delta\mathbf{V}_{DSM(i)} &= \Delta\mathbf{V}_{DSM(i)}\left(\mathbf{V}_{\infty(i)}, B_{(i)}, t_{DSM(i)}, t_i\right) \end{aligned} \tag{4.7}$$

With:

$$B_{(i)} = \left\lfloor \phi_{(i)}, r_{p(i)} \right\rfloor \tag{4.8}$$

And:

$$\mathbf{V}_{\infty(i)} = f\left(t_i, t_{DSM(i-1)}, \mathbf{r}_{DSM(i-1)}, t_{DSM(i)}, \mathbf{r}_{DSM(i)}\right) \tag{4.9}$$

And where t_0 is the departure date, t_f is the arrival date, t_i are the date of planet encounter, $t_{DSM(i)}$ are the DSM date, and $\mathbf{r}_{DSM(i)}$ are the DSM position.

And the decision vector is:

$$\mathbf{X} = \left\lfloor t_0, V_0, \alpha_0, \beta_0, t_{DSM(1)}, ..., t_i, B_{(i)}, t_{DSM(i)}, ..., t_{n-1}, B_{(n)}, t_{DSM(n)}, t_f \right\rfloor$$

Clearly the problem is not separable. The ΔV depend on more than one variable, so is for their derivatives, and these variables are common to other ΔV .
It is however possible to make the ΔVs independent. As we propose in the following section, we can use additional variables which a priori do not provide additional information. Indeed, these variables can decouple the problem and make the problem separable. The optimization of the overall problem can be decomposed in the optimization of several sub-problems as it was the case in the preceding section 3.

4.2.2 Formulation of the sub-problems

Now applying the above decomposition to the transfer, we can use the variables, such that:

$$\begin{aligned}\Delta\mathbf{V}_0 &= \Delta\mathbf{V}_0\left(t_0, \tilde{t}_{DSM(1)}, \tilde{r}_{DSM(1)}\right)\\ \Delta\mathbf{V}_f &= \Delta\mathbf{V}_f\left(t_f, \tilde{t}_{DSM(n)}, \tilde{r}_{DSM(n)}\right)\\ \Delta\mathbf{V}_{DSM(i)} &= \Delta\mathbf{V}_{DSM(i)}\left(\tilde{B}_{(i)}, t_{DSM(i)}, t_i\right)\end{aligned} \tag{4.10}$$

With:

$$\begin{aligned}\mathbf{B}_{(i)} &= \left[V_{\infty(i)}, \phi_{(i)}, r_{p(i)}\right]\\ \tilde{\mathbf{B}}_{(i)} &= \left[\tilde{V}_{\infty(i)}, \tilde{\phi}_{(i)}, \tilde{r}_{p(i)}\right]\end{aligned} \tag{4.11}$$

The variables $\tilde{\mathbf{B}}_{(i)}$ are a duplication of their equivalent variables $B_{(i)}$. They represent the swing-by conditions. They can be directly and explicitly related to the swing-by hyperbolic velocity vectors $\mathbf{V}_{\infty(i)}$.

And the decision vector is indeed:

$$\mathbf{X} = \left[\underbrace{t_0, V_0, \alpha_0, \beta_0, t_{DSM(1)}, \tilde{\mathbf{B}}_{(i)}, \tilde{t}_1}_{\text{initial leg}}, \ldots, \underbrace{t_i, \mathbf{B}_{(i)}, t_{DSM(i)}, \tilde{\mathbf{B}}_{(i+1)}, \tilde{t}_{i+1}}_{\text{leg n°i}}, \ldots, \underbrace{t_{n-1}, \mathbf{B}_{(n)}, t_{DSM(n)}, t_f}_{\text{final leg}}\right] \tag{4.12}$$

with $i = 1 \ldots n-2$.

The redundant variables must coincide, and then we have of course:

$$\begin{cases}\tilde{\mathbf{B}}_{(i)} = \mathbf{B}_{(i)}\\ \tilde{t}_i = t_i\end{cases} \tag{4.13}$$

These are the expression of the matching condition for each duplicated variable.

Assumption 4.1:
To simplify the search process, we removed the constraint on the angular deviation of the swing-by. This allows removing α_f, β_f from the decision vector.

Thus we cannot check if the swing-by is feasible or not and may compute swing-by infeasible trajectories. But this is easily solved when we patch the legs together to construct complete transfer.

For our space trajectory optimization problem, the decision vector for each leg is then:

$$\mathbf{X}_i = \left[t_i, t_{DSM(i)}, t_{i+1}, \mathbf{V}_{\infty 0 i}, V_{\infty f i}\right]$$

Where:

- t_{0i} is the departure date for the single leg
- t_{dsm} is the date of the Deep Space Manoeuvre (DSM)
- t_{fi} is the arrival date for the single leg
- $V_{\infty i}$ is the hyperbolic excess velocity at departure of the leg
- $V_{\infty fi}$ is the hyperbolic excess velocity upon arrival

We use the same description for each leg. This is detailed on Figure 22.

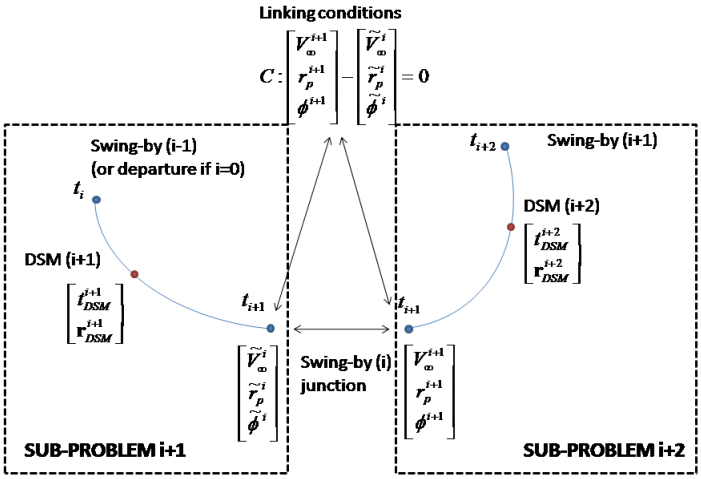

Figure 22. MGADSM partionning

4.2.3 Solving the problems

The simplify the solving of the sub-problems, let's consider discrete and continuous variables of the sub-problem decision vector.
The discrete variables are:

$$\mathbf{x}_G = \left\lfloor t_0, t_{DSM}, t_f, V_{\infty 0}, V_{\infty f} \right\rfloor_{legi}$$

The continuous variables are:

$$\mathbf{x}_l = \left[\alpha, \beta\right]_{legi}$$

The local problem to solve once x_G is given is:

$$\min_{\mathbf{x}_l} \Delta V_{DSM}\left(\mathbf{x}_G, \mathbf{x}_l\right) \tag{4.14}$$

Under the constraint:

$$\psi = \left\| \mathbf{V}_{\oplus f} - \mathbf{V}\left(t_f\right) \right\| - V_{\infty f} \tag{4.15}$$

Where $\mathbf{V}_{\oplus f}$ is the arrival planet velocity at t_f. Indeed, $V_{\infty f}$ is a constraint for the leg. The vector $\mathbf{V}_{\infty 0} = [V_{\infty 0}, \alpha_0, \beta_0]$ is an initial condition for the leg. It can also describe the output of a swing-by manoeuvre.

This local problem must be solved for all points of the map defining $\mathbf{x}_G$.

Remark:
We now have to solve M problems in a search space of dimension N, whereas in the initial approach we solved 1 problem in a search space of dimension $4M+2$*, where M is the number of phase, and N is the size of the decision vector for each sub problems* $(N=9)$.

This approach starts to be beneficial when M>1, but the benefits become great for high number of legs.
More importantly, with this approach we did not make any assumption that would prevent us from finding the global optimum, except that we constraint the body to body legs to have exactly one DSM.

This approach permits to apply pruning methods on the sub problems, before constructing the solution. In addition the complexity is reduced compared to the initial problem.

4.2.4 Scheme

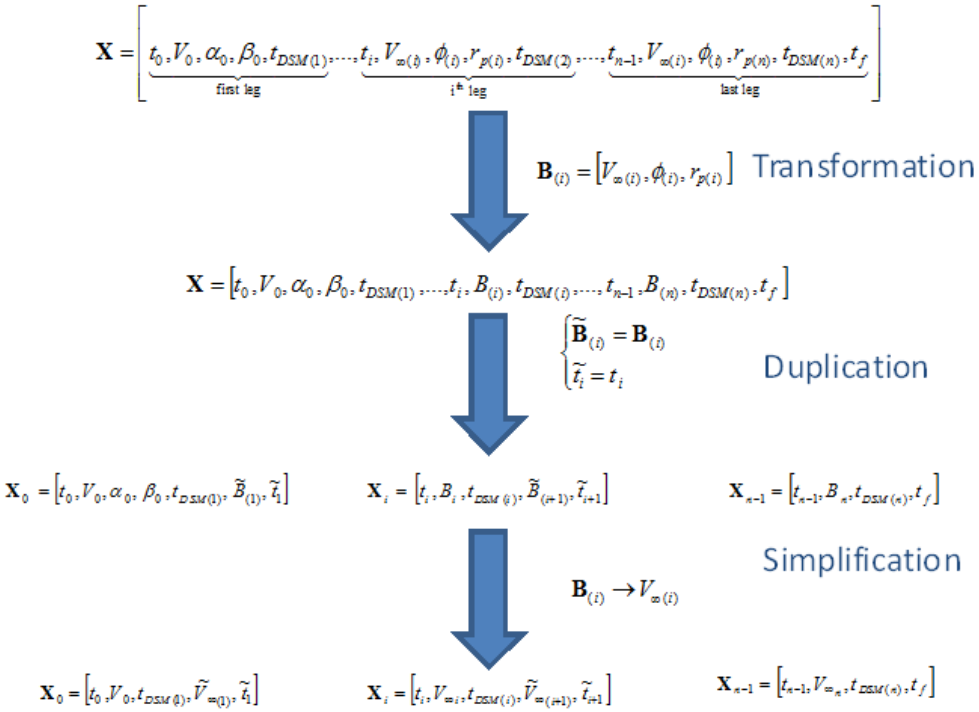

Figure 23. Splitting Scheme

4.2.5 Complexity

For each phase, consider the following grid:

Variable	Number of bins
T_0	k
Tof	k
t_{DSM}	j
$V_{\infty 0}$	n
$V_{\infty F}$	n

Each phase has thus the following complexity: $C_i = jk^2n^2$.

However, as we use the same discretization for T_0 and *tof*, if the first phase has *k* bins on T_0 and *tof* the second phase has *2k* bins, the third has *3k* bins, etc … Indeed, each phase contributes to increase the T0 space by adding k new bins.

The overall complexity can then be written:

$$C = \sum_{i=1}^{N} iC_1 = N\frac{N+1}{2}jn^2k^2 \tag{4.16}$$

Where N is the number of phase, a phase being the transfer between 2 consecutive planets in the sequence.

4.2.6 Pruning

Assumption 4.2:
We suppose we find the global optimum of each sub problems for the different boundary condition.

This assumption is important if we want to prune the correct part of the space. Indeed, for a given set of interior point boundary conditions, the global optimum is described by the global optimum of each sub problems. This can easily be proved considering the cost is additive and we have unpowered swing-bys.

We have 6 pruning strategies:

1. *Initial hyperbolic excess velocity pruning*: We can prune the space with the boundary on the global variables, for $V_{\infty 0}$ for the initial and final leg.
2. *Final hyperbolic excess velocity pruning:* We can prune the space with the boundary on the global variable $V_{\infty f}$ for the final leg.
3. *Time of flight pruning*: It is also possible to allow a minimum time of flight for each leg (transfer between 2 subsequent planets of the scenario).

4. *Swingby pruning* We can allow a minimum V_∞ for the swingby.
5. *DSM ΔV pruning* : We can prune leg with a DSM ΔV above a given limit. This permit also to remove point of the next phase matching according to $V_{\infty 0}, T_0$.
6. *Forward pruning*: if on the phase i there is no solution arriving at a given date on the planet *i*, we remove the date as a launch date for the phase *i+1*. The same apply on the velocity.

To improve convergence of the local solver, we allow a tolerance on $V_{\infty f}$ and provide accurate gradient using the development of 2.5.

It is likely that most of the pruning is done on the initial and final phase. Pruning on the intermediate phases can merely be done through the *Time of flight,* the *DSM ΔV* and the *Forward pruning.*

4.2.7 Discussion

It is important to be sure that this scheme is consistent with the global optimization problem, i.e. that the optimum found is effectively at least an optimum of the whole trajectory problem.

To allow this, we actually added a constraint ψ (10) which permit to « communicate » between the leg (this is similar to the interaction prediction principle). In forward direction, all subsequent legs need to know the V_∞ which permit to have a feasible swing-by or eventually evaluate a post swing-by correction manoeuvre.
Since we do not take care about the rotation of the $\mathbf{V}_\infty$ vector, and since we evaluate different values of $V_{\infty f}$ and take the best optimum for each local problem (9), we do not miss solutions.

4.3 Applications

4.3.1 EM transfer

Table 17.
EM DSM-GASP variables bounds and constraints

	EVM transfer		
Variable	**Lower limit**	**Upper limit**	**Step size**
T_0 (days)	01/01/2001	01/06/2004 +300	10
T (days)	100	300	10
V (m/s)	500	15000	500
Constraints			
V_{0max} (m/s) (PRUNE 1)	3000		
V_{fmax} (m/s) (PRUNE 2)	5000		
T_{min} (days) (PRUNE 3)	100	On the leg length	
T_{max} (days) (PRUNE 3)	250	On the leg length	
ΔV_{DSM} (m/s) (PRUNE 4)	Inf		
Tolerance on ΔV_{DSM} (m/s) (PRUNE 4)	250	ΔV_{DSM} +/- tol	
Local Opt. Max Nb. Iteration (PRUNE 4)	300		

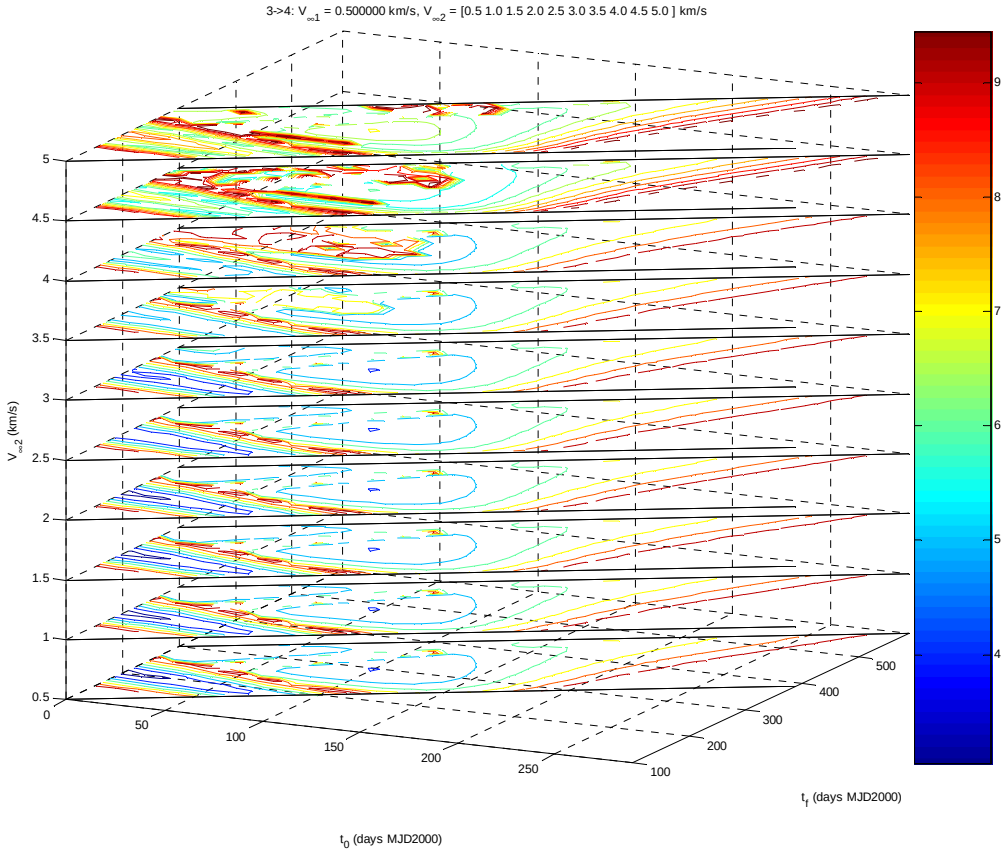

Figure 24. Example of slice contour for EM transfer with $V_{\infty 1}$ = 0.5 km/s, sum of ΔV < 10 km/s.

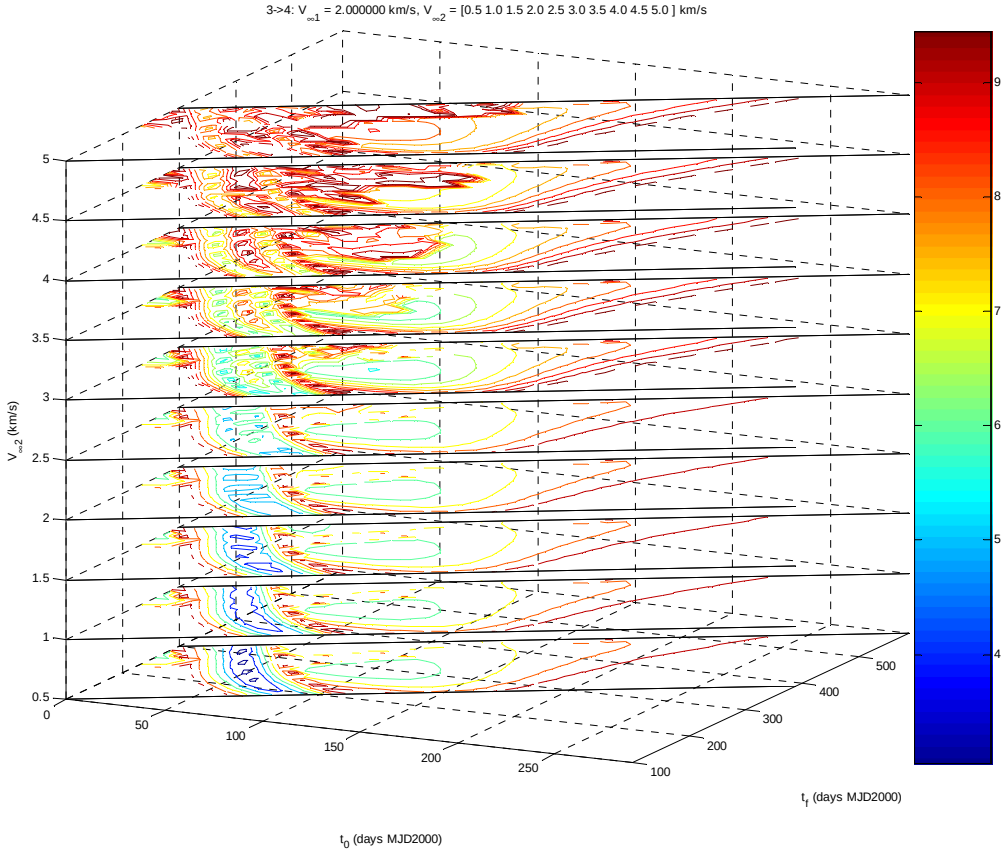

Figure 25. Example of contour slice for EM transfer with $V_{\infty 1}$ = 2km/s, sum of ΔV < 10 km/s.

4.3.2 EVM transfer

Table 18.
EVM DSM-GASP variables bounds and constraints

EVM transfer **Variable**	**Lower limit**	**Upper limit**	**Step size**
T_0 (days)	01/06/2004	01/06/2004 +100	10
T (days)	180	250	10
V (m/s)	500	10000	500
Constraints			
V_{0max} (m/s) (PRUNE 1)	3000		
V_{fmax} (m/s) (PRUNE 2)	5000		
$V_{\infty max}$ (m/s) (PRUNE 1)	8000	Minimum V∞ for swing-by	
T_{min} (days) (PRUNE 3)	140	On the leg length	
T_{max} (days) (PRUNE 3)	250	On the leg length	
ΔV_{DSM} (m/s) (PRUNE 4)	Inf		
Tolerance on ΔV_{DSM} (m/s) (PRUNE 4)	250	ΔV_{DSM} +/- tol	
Local Opt. Max Nb. Iteration (PRUNE 4)	100		

On a Pentium 3Ghz computer, 1Gb RAM, running MATLAB® under Windows XP, this example took about 3h40 of computation time.
However, after the computation, we have a complete map on which we can apply the pruning policy. We do not need to compute again the map if we change the pruning parameters.

Best solution on the grid:

Table 19.
EVM DSM-GASP best grid solution

EVM transfer **Event**	**date**	**Comment**
T_0	T0=2453097.5	V_∞ = 2 km/s
T_{dsm} 1	T0+18	
T_1	T0+180	(Swingby) V_∞ = 6.0 km/s
T_{dsm} 2	T0+205 (T1+125)	
T_f	T0+430 (T1+250)	V_∞ =4.5 km/s
TOTAL	**430 days**	**8.94 km/s**

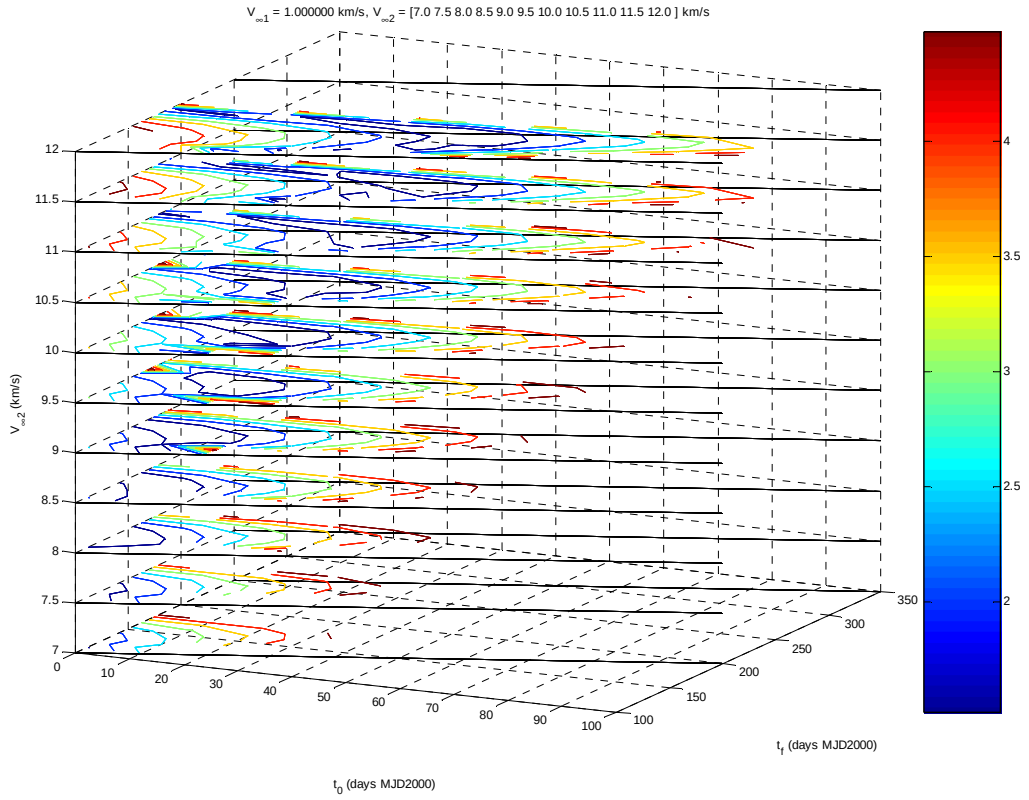

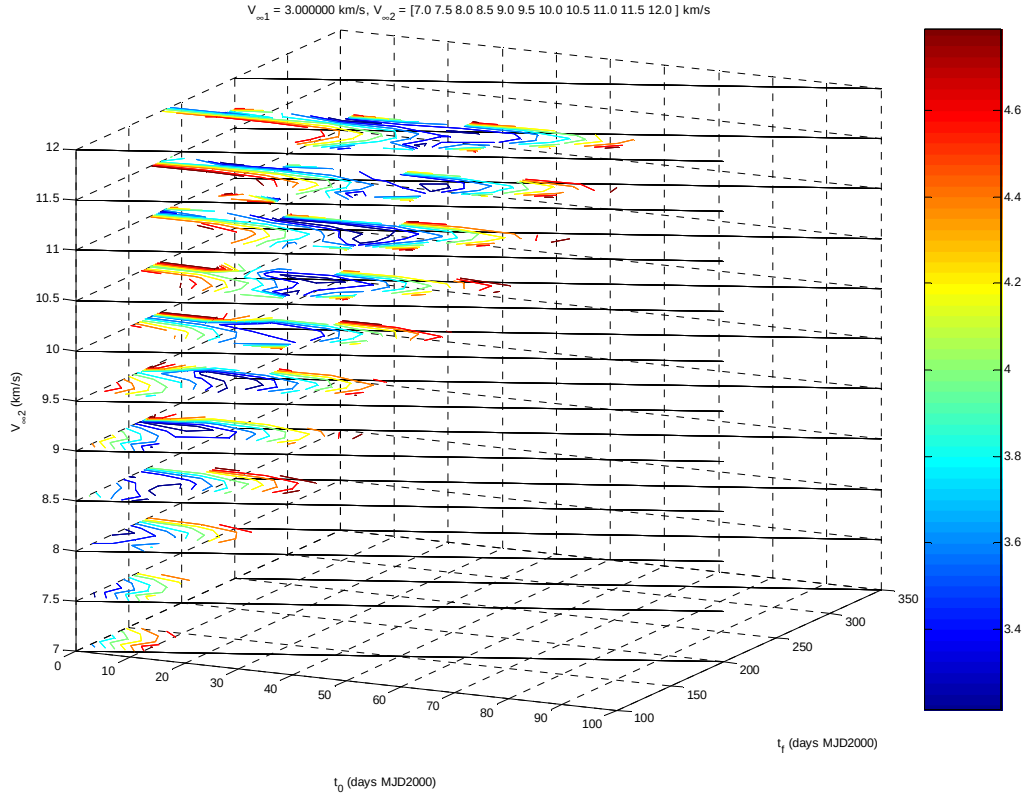

Figure 26. EVM, phase EV, $\Delta V_0+\Delta V_{DSM} < 5$km/s

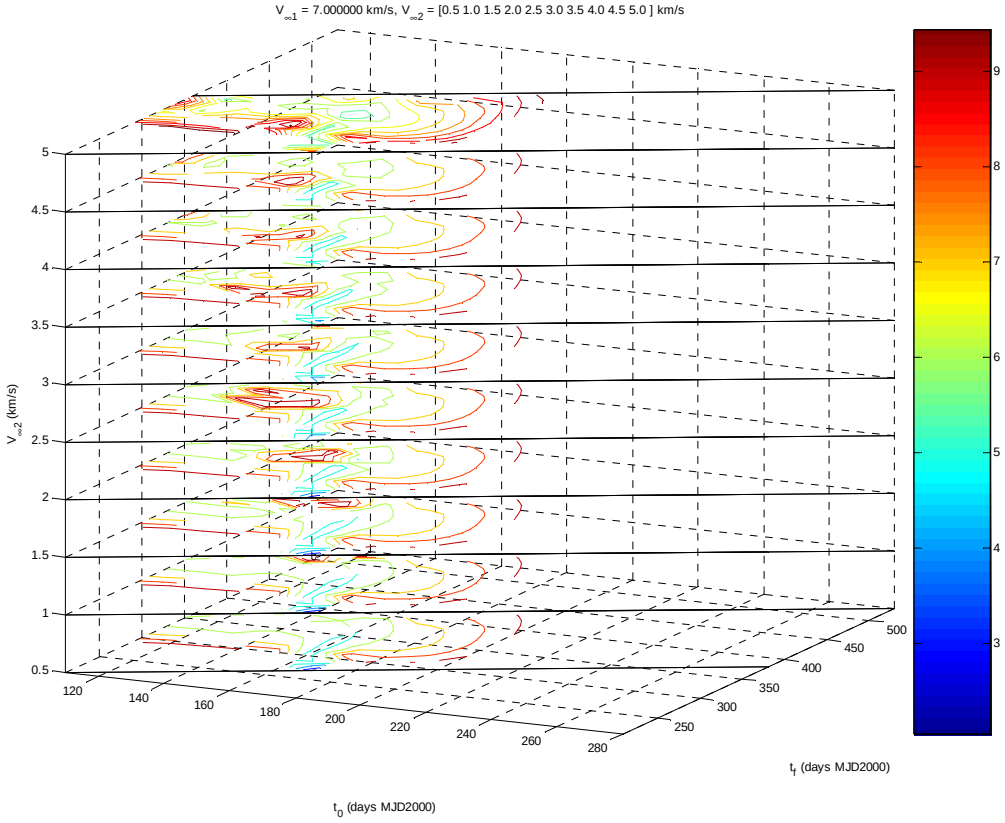

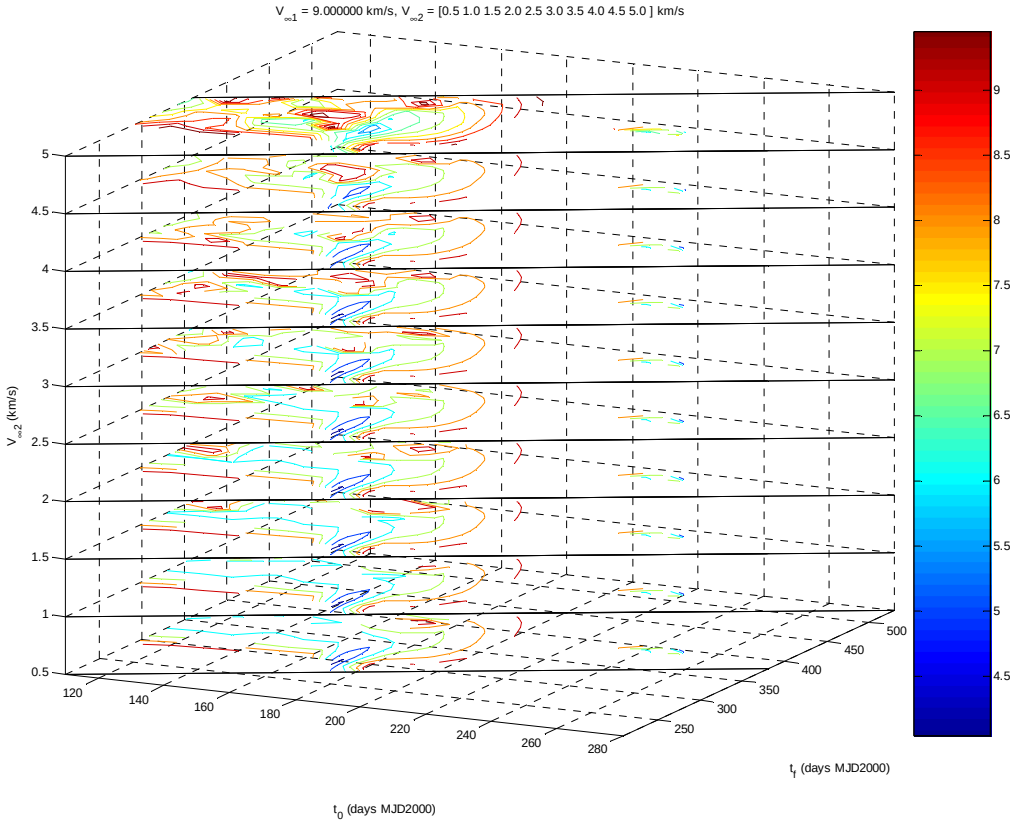

Figure 27. EVM, phase VM, $\Delta V_{DSM} + \Delta V_F < 10$ km/s

As we computed all possible legs on the grid, we also computed the extremals on the global optimum.

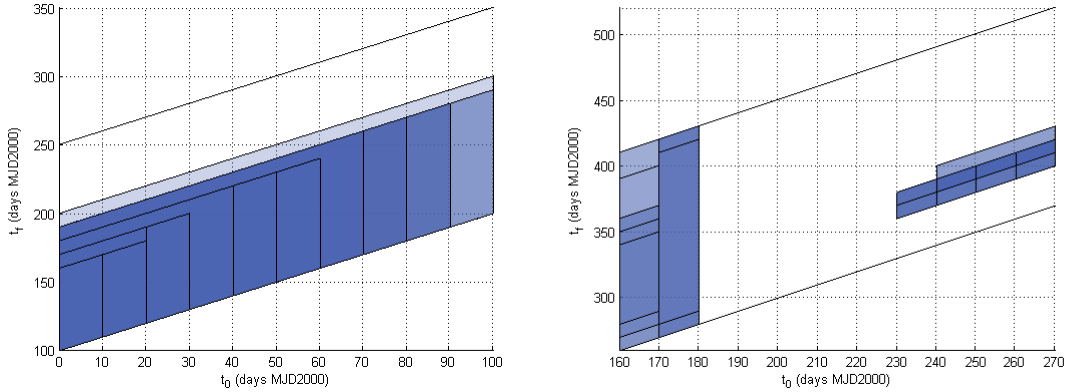

Figure 28. EV phase (ΔV<5 km/s, 66 boxes) and VM phase (ΔV<5 km/s, 159 boxes), Pruned space

Of course this is not a good representation as some boxes are superimposed and the display lack information on the subspace that contains this boxes. However, this is still the most intuitive one.
The darker the colour, the more superimposed boxes there are.
A more accurate representation would be like these one:

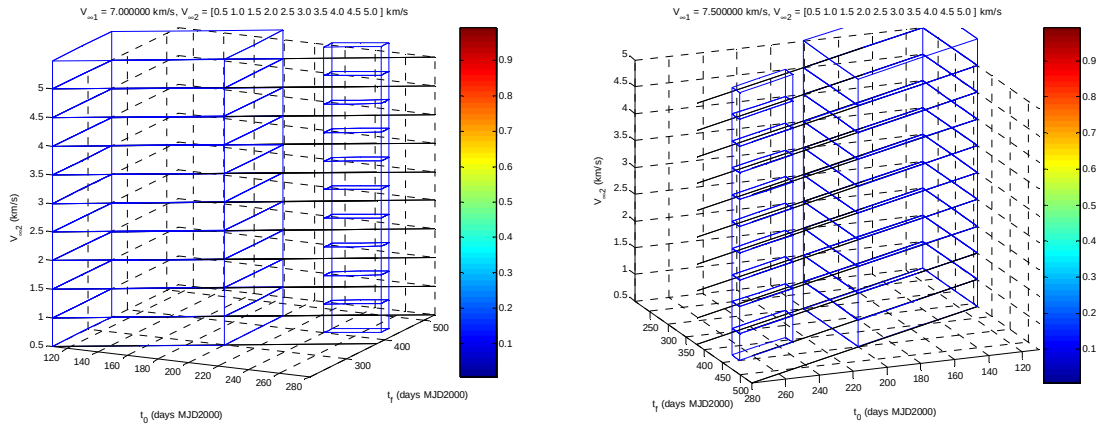

Figure 29. Multi-D representation of the non pruned space.

On Figure 29 we only displayed 2 projections of the multidimensional solution space.

4.3.3 EVEJ transfer

Table 20.
EVEJ DSM-GASP variables bounds and constraints

EVEJ transfer **Variable**	**Lower limit**	**Upper limit**	**Step size**
T_0 (days)	4745	5840	10
T (days)	100	1000	20
V (m/s)	500	10000	500
Constraints			
V_{0max} (m/s) (PRUNE 1)	3000		
V_{fmax} (m/s) (PRUNE 2)	5000		
$V_{\infty max}$ (m/s) (PRUNE 1)	10000	Minimum V∞ for swing-by	
T_{min} (days) (PRUNE 3)	[100, 300, 1000]	On the leg length	
T_{max} (days) (PRUNE 3)	[200, 400, 1000]	On the leg length	
ΔV_{DSM} (m/s) (PRUNE 4)	Inf		
Tolerance on ΔV_{DSM} (m/s) (PRUNE 4)	250	ΔV_{DSM} +/- tol	
Local Opt. Max Nb. Iteration (PRUNE 4)	300		

Table 21.
EVEJ DSM-GASP statistics

EVEJ transfer **Statistic**	**value**
Solver calls	3138762
Ephemeris Gen. calls	295
Local Solution for phase[1]	57553
Local Solution for phase[2]	348872
Local Solution for phase[3]	671526

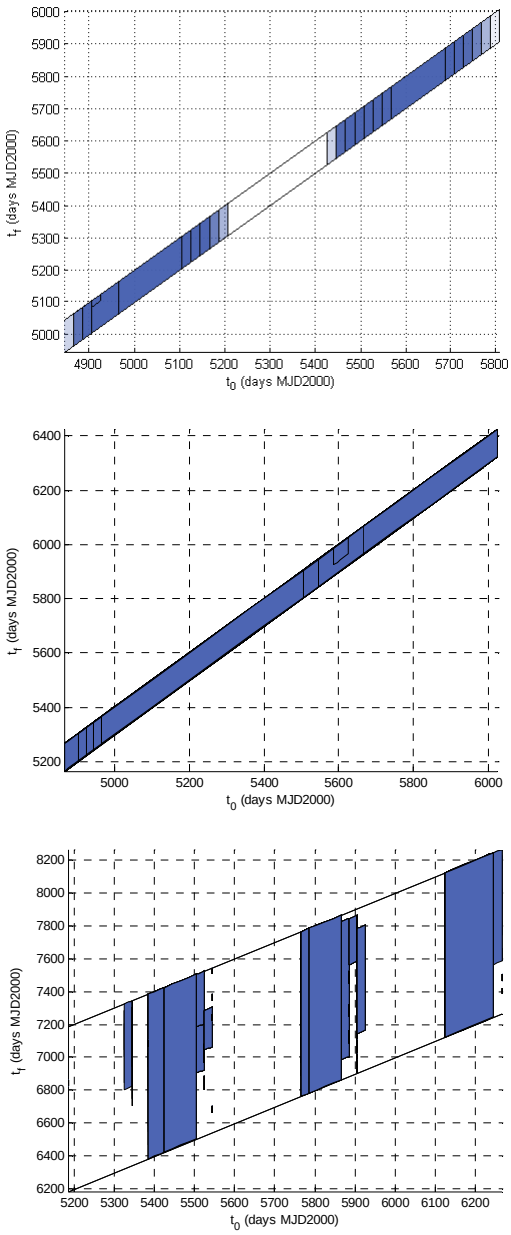

Figure 30. EV (ΔV<5km/s, 145 boxes), VE (ΔV_{DSM}<3km/s, 637 boxes), EJ (ΔV<3km/s, 1085 boxes)

On this example, and despite the ΔV_{DSM} pruning constraint the phase 2 appears to be a low energetic part. We hardly manage to prune the space. Remember however, that the method do not make any assumption in the pruning process or the map construction. It is a true representative of the real map.

4.4 Conclusions

We demonstrate that under weak assumption the problem complexity can be polynomial and of order 5. The complexity is polynomial with respect to the discretization and the variable used. We can compute MGADSM which any number of phase with a quite reasonable computational cost, even though one might emphasize that the polynomial exponent is still high and only advance in computer design and engineering can give reasonable computational time (< day) for a preliminary design tool. It is likely that the complexity cannot be further decrease unless under strong assumptions.
A strong drawback of this approach is the possible non feasibility of the swing-by. In order to reduce the complexity and the dimension of the search space from 9 to 5, we make a assumption that does not permit to ensure the swing-by feasibility. But this can be check out when constructing a trajectory or pruning decision vector space.
Going back to the 9 dimension formulation can give more usable results, but as a preliminary approach we consider that the swing-by feasibility is not a major concern has we can still prune the non feasible solution. Note that the approach does permit to find also all the feasible solution on the search space grid.

5 Conclusions

In this study we tried to propose different approaches to tackle the problem of multiple gravity assist – deep space manoeuvre (MGADSM) space pruning problem.

We first introduce the primer vector theory for direct planet to planet transfer, and then extend the theory to multi gravity assist trajectories. The method allows to automatically find the optimal deep space manoeuvres (DSM), as well as their optimal number. As shown with the example, the decision vector is in this case reduced to the dates of encounter with the planets. Although the method has a linear convergence and uses local optimization techniques, it performs well and managed to find the good solutions.

Following an experimental intuition, we then tried to use a local – global approach. Our intuition told us that some part of the decision vector can be optimized locally, whereas the remaining part needs a global optimization scheme. This approach permits to remove the "hard" part of the decision vector to the global optimization algorithm. The examples show that this approach, when used with a heuristic algorithm like Differential Evolution (DE) permits to reduce the search space for each chromosome (or particle), and then ease the search for an optimal solution.

The last approach followed was in part inspired by the GASP algorithm and the decomposition – coordination algorithm expressed earlier. Indeed, it splits up the problem into sub problems. Each sub problems can then be solved independently if we span different boundary conditions. When each sub problem has produced the set of potential extremals, we patch each sub solution according to specific boundary conditions to construct a complete trajectory. This also permits to efficiently prune the solution space, as we can constraint the hyperbolic excess velocity, the DSM amplitude for each leg, the dates, ….
As the decision vector size for each sub problem is reduced compared to the decision vector size of the complete problem, we reduce the complexity as well. We demonstrated that we have a polynomial complexity.

Each of the 3 approaches brings a solution to the initial question of MGADSM space pruning. However, they should all be improved by speeding up the convergence of the local optimization process. All of the approaches proposed need an efficient local optimization algorithm, and manage to find a solution even for harsh problems.

References

[1] R.H. Battin, *An introduction to the Mathematics and methods of Astrodynamics*, AIAA Eduation series.

[2] D. Izzo, V.M. Becerra, D.R. Myatt, S.J. Nasuto, J.M. Bishop, *Search Space Pruning And global Optimisation of Multiple Gravity Assist Spacecraft Trajectories*, accepted for publication in Journal of Global Optimisation 2006.

[3] V.M. Becerra, D.R. Myatt, S.J. Nasuto, J.M. Bishop, D. Izzo, *An Efficient Pruning Technique for the Global Optimisation of Multiple Gravity Assist Trajectories*, Proceedings of Global Optimisation 2005.

[4] D.R. Myatt et al., *Advanced Global optimisation for Mission Analysis and Design*, ESA, 2003.

[5] F. Peralta, S. Flanagan, *Cassini Interplanetary Design*, TO COMPLETE

[6] J. Schoenmaekers, R. Bauske, *Re-design of the Rosetta mission for launch in 2004*, Proceedings of the 18th International Symposium on Space Flight Dynamics, DLR-ESA/ESOC, 11-15 October 2004, Munich, Germany.

[7] D.J. Jezewski, *Primer Vector Theory and applications*, NASA, 1975

[8] Guzman, Mailhe, *Primer Vector Optimization Survey of Theory*, New analysis and Applications, 53rd International Astronautical Congress, Houston 2002

[9] D.J. Jezewski, H.L. Rozendaal, *An efficient Method for Calculating optimal Free Space N-Impulse Trajectories*, AIAA Journal, Vol.6 No.11, 1968

[10] D.R. Glandorf, *Primer Vector Theory for Matched-Conic Trajectories*, AIAA Journal, Technical Notes, Vol.8 No.1, January 1970.

[11] M.S. Konstantinov, G.G. Fedotov, V.G. Petukhov, ACT Global Optimization Workshop, ACT-ESA 2005.

[12] R.D. Sugar, A.R. Stubberub, *Decomposition Technique for Minimum Time Trajectories*, Journal of Optimization and Applications, Vol.14, No.2, Aug 1974, p233-250

[13] G. Cohen, B. Miara, *Optimization with an Auxiliary constraint and decomposition*, SIAM journal of Control and optimization, 28, 137-157, 1990.

[14] A.E. Petropoulos, *A shape based approach to automated, low thrust, gravity assist trajectory design*, PhD thesis, Purdue university, 2001.

[15] D. Izzo, *Lambert's problem for exponential sinusoids*, ACT/ESTEC internal report ACT-RPT-4100-DI-LMSP01, april 2005.

[16] J. Navagh,*Optimizing interplanetary trajectories with deep space maneuvers*, M.S. Thesis George Washington Univ, 1993.

[17] J. Kennedy, R. Eberhart, *Particle Swarm Optimization*, Proc. IEEE Intl.Conf. on Neural Networks, 1995.

[18] J.T. Betts, *Survey of Numerical Methods for trajectory Optimization*, Journal of Guidance Control and Dynamics 1998, Vol. 21, no. 2.

[19] T.T. McConaghy, T.J. Debban, A.E. Petropoulos, J.M. Longuski, *Design and optimization of Low thrust trajectories with gravity Assists*, Journal of Spacecraft and Rockets, Vol. 40, No. 3, 2003.

[20] T.J. Debban, T.T. McConaghy, J.M. Longuski, *Design and optimization of low thrust gravity assist trajectories to selected planets*, AIAA/AAS Astrodynamics Specialist Conference and Exhibit, August 2002.

[21] Antonio de Almeida Prado ,*Powered swing by*, AIAAJournal of Guidance, Control, and Dynamics 1996.

[22] J. C. Niehoff, *Gravity-assisted trajectories to solar-system targets*, J. of Spacecraft and Rockets, 1966, vol.3 no.9
[23] Interplanetary Mission Design Handbook, *Earth To Mars ballistic Mission opportunity*, JPL publication 82-43, Volume 1, Part 2.
[24] D.W. Parcher, J.A. Sims,*Venus and Mars Gravity Assist Trajectoeris to Jupiter Using Nuclear Electric Propulsion*, AAS 05.
[25] D.W. Parcher, J.A. Sims, *Gravity-assist trajectories to Jupiter using nuclear electric propulsion*, 2005 AAS/AIAA Astrodynamics Specialist Conference.
[26] A.E. Petropoulos, J.M. Longuski, E.P. Bonfiglio, *Trajectories to Jupiter via Gravity Assist from Venus, Earth and Mars*, J. of Spacecraft and Rockets, Vol. 37, No. 6, 2000.
[27] C.H. Yam, T.T. McConaghy, K.J. Chen, J.M. Longuski, *Design of Low Thrust Gravity Assist Trajectories to the Outer Planets*, IAC 2004.
[28] N.J. Strange J.M. Longuski, *Graphical Method for Gravity Assist Trajectory Design, Journal of Spacecraft and Rockets,* Vol. 39, No. 1; January 2002.
[29] A.E. Petropoulos and J. Sims, *A review of Some Exact Solutions to the Planar Equations of Motion of a Thrusting Spacecraft*, Proceeding of 2nd International Symposium on Low Thrust Trajectories, 1995.
[30] D.L. Matson, L.J. Spilker, JP. Lebreton, The Cassini/Huygens Mission to the Saturnian System, Space Science Reviews, Vol. 104, p.1-58, 2002
[31] S.P. Hughes, L.M. Mailhe, J.J. Guzman, *A Comparison of trajectory optimization for the Impulsive minimum Fuel Rendezvous Problem*, Advances in the Astronautical Sciences, Guidance and Control 2003, Breckenridge 2003
[32] P. DePascale, M. Vasile, *Preliminary Design of Multiple Gravity Assist trajectories*, Journal of Spacecraft and Rockets, Vol. 42, No. 4, 2006
[33] G. Cohen, *Optimization by Decomposition and Coordination: A unified Approach*, IEEE transaction on automatic control, Vol. 23, No. 2, April 1978
[34] Bryson, A., Ho, Y.C., Applied Optimal Control, Hemisphere Publishing, New York, 1975.

List of Figures

List of Tables

INDEX